IEEE Access
Multidisciplinary ⋮ Rapid Review ⋮ Open Access Journal

Received May 5, 2022, accepted May 29, 2022, date of publication June 8, 2022, date of current version June 16, 2022.

Digital Object Identifier 10.1109/ACCESS.2022.3180835

Performance Evaluation of LDPC-Coded Power Series Based Málaga (Ḿ) Distributed MIMO/FSO Link With M-QAM and Pointing Error

D. ANANDKUMAR, (Member, IEEE), AND R. G. SANGEETHA, (Senior Member, IEEE)
School of Electronics Engineering, Vellore Institute of Technology, Chennai Campus, Chennai 600127, India
Corresponding author: R. G. Sangeetha (sangeetha.rg@vit.ac.in)

ABSTRACT In this work, the performance evaluation of Low-Density-Parity-Check (LDPC) based Multiple Input Multiple Output (MIMO) Orthogonal Frequency Division Multiplexing (OFDM) based Free Space Optical (FSO) link with Málaga (Ḿ) channel model is analyzed. The performance in terms of Gain (diversity and combining) analysis δG (N, M) and Bit Error Rate (BER), outage probability, ergodic capacity, spectral efficiency and Link distance (L) concerning Signal to Noise Ratio (SNR) is evaluated. The Meijer-G function gives complexity in MIMO mathematical analysis. As a solution, a new Probability Density Function (PDF) based on power series representation has been proposed with M-Quadrature Amplitude Modulation ($M-ary\ QAM$). With the proposed PDF, the closed-form Bit Error Rate (BER) derivation, Asymptotic BER derivation, Outage probability expression are derived, and the enhancement is observed for the MIMO/OFDM link in terms of Bit Error Rate (BER) and Signal to Noise Ratio (SNR) with pointing error (PE) and atmospheric turbulence (AT). The Maximal Ratio Combining (MRC) achieves a gain of 3.5dB and 7.8dB SNR gain over Equal Gain Combining (EGC) and Selection Combining (SC) scheme for negligible Pointing Error (PE), i.e., $\xi = 10.15$ at BER 10^{-6}. The proposed PDF, along with M-QAM and Málaga (Ḿ) distribution offers power efficiency, reduction in BER, and high SNR gain compared to Single Input Single Output (SISO) and Single Input Multiple Output (SIMO) Free Space Optical (FSO) link. The regular LDPC coding techniques are adopted with a 1/2 code rate and applied to simulation results to obtain high coding gain. The proposed MIMO/FSO link provides high SNR gain of 5dB and transmission link distance of 12km over SIMO and SISO FSO link. This work gives the in-depth analysis of vital factors affecting the FSO link performance and helps in mitigating them to analyze and design an effective system and opens widely for digital applications like smart city application, 5G and beyond 5G, Internet of Things (IoT), railway and defense applications, etc.,

INDEX TERMS Málaga (Ḿ), ($M-ary\ QAM$), pointing error, atmospheric turbulence, power series, BER, SNR, gain.

I. INTRODUCTION

Due to the high bandwidth, unlicensed spectrum, higher data rate, excellent security, and low-cost implementation, the Free Space Optics (FSO) attracts more attention in communication research [1], [2]. Despite many advantages, the atmospheric turbulence dependency is the main disadvantage, leading to complete link loss and the line of sight problem between the transceivers [3]. The intensity-modulated direct detection (IM/DD) is not preferred to overcome the issue because of the high bit error rate. The subcarrier intensity modulation (SIM) suits well compared to IM/DD due to better error performance with Atmospheric Turbulence (AT) and Pointing Error (PE) [4]. The SIM, along with higher modulation techniques, Phase Shift Keying (PSK) and M-ary Quadrature Amplitude Modulation ($M-ary\ QAM$), gives better BER and higher data rate [5]. The FSO link performance is primarily degraded due to AT and PE compared to scintillation, scattering, and absorption effects. The building sway introduces the pointing error and needs to be considered for a better analytical study of the FSO link [5].

However, the outdoor FSO link is mainly degraded by atmospheric factors like snow, fog, rain, and other man-made particles that attenuate the optical signal. The attenuation

The associate editor coordinating the review of this manuscript and approving it for publication was Ke Guan.

primarily occurs with AT and adverse effects because of temperature, pressure, and refractive index changes, leading to the limitation of FSO communication, especially outdoor FSO links to few hundreds of meters [5]. Techniques like aperture averaging, cooperative communication, Multiple Input Multiple Output (MIMO), adaptive optics, coding techniques, and SIM-based advanced modulation formats can also improve the data rate, reduce error rate, and increase communication link distance. In [6] and [7], the effect of PE is reduced using single-input multiple-output (SIMO) with Maximal ratio combining (MRC) and Gamma-Gamma channel model. In [8], it speaks much about SIMO under log-normal distribution with PE, but MIMO is a spatial diversity technique that uses multiple transmitters to provide independent paths in the atmosphere to improve the system performance under strong AT regime [9]. Reception is carried out with various combining schemes like Maximal ratio combining (MRC), Equal Gain Combining (EGC), and Selection Combining (SC) [9]. The SC schemes [9]–[11] and PE [9]–[13] are not considered in most of the surveys, and in-depth analysis of this gives a better analytical understanding and realistic study of the FSO link. In [9], SC gives more or less equal BER performance with K-distribution and ON-OFF Keying (OOK) modulation compared to EGC with Intensity modulated/Direct Detection (IM/DD). For instance, in [10], Duo-Binary Phase Shift Keying (DB-PSK) and SIM-based Differential- Phase Shift Keying (D-PSK) with PE is studied and SC is not considered.

The perfect analytical study of light intensity selection and scintillation effects is carried out with SC, which outperforms EGC. In [14], the log-normal distribution along with SC and OOK modulation without PE is analyzed for real-time scenarios of the FSO link. Considering suitable modulation schemes and channel models, an Orthogonal Frequency Division Multiplexing (OFDM) along with SIM modulation techniques like M-ary Quadrature Amplitude Modulation ($M - ary\ QAM$), Quadrature PSK (QPSK), M-ary PSK (M-PSK) are used commonly in innovative applications including 5G (fifth generation), High Definition (HD), Railway and defense applications [15]. In OFDM, no equalizations are required because it uses Inverse Fast Fourier Transform (IFFT) for the generation of the signal and Fast Fourier Transform (FFT) for the reception of the signal. The number of sub-carriers are used for high data rate because of the split of data rate into lower bit streams and passed over the atmosphere, which gives high spectral efficiency and ergodic capacity [16]. The clipping or Direct Current (DC) biasing is used to remove the negative cycle of the optical signal because it will be in uni-polar nature and makes the optical signal suitable for transmission by Light Emitting Diode (LED) or Laser diodes [17].

In RF, the bandwidth is limited, but in FSO, it is unlimited. To avail the high bandwidth and high rate data rate, OFDM and MIMO is the suitable candidate for future generation wireless applications, Internet of Things (IoT), and smart applications [18]. The system with MIMO-OFDM performs better for efficient outdoor FSO link, the MIMO-OFDM-based study is an important direction for future generation applications. Forward error correction (FEC) techniques also play a significant role in FSO link design because of the errors produced by communication media. FEC techniques like Reed-Solomon, Turbo codes (TC), low density parity check (LDPC) enhances the FSO and RF link performance. The LDPC is primarily used in telecommunication fields, i.e., wireless [19]. In [20], the literature shows the effects of LDPC-SISO with OFDM with AT [20]. The LDPC-MIMO with AT and experimental setup of OFDM-based SISO is studied [21] and [22]. The MIMO with log-normal and GG fading channel also studied with average capacity in [23]. These papers are dealt with MIMO-OFDM schemes without any coding techniques and report on spatial diversity analysis [24].

Many conventional stochastic channel models, such as Gamma-Gamma, and Log-normal, are investigated in the literature. The advanced channel models like Geometric based stochastic modeling (GBSM) and mm-wave channel models are discussed in detail [25]–[27]. However, the outdoor applications are not explored. It's designed for multipath fading in the indoor environment, but the outdoor terrestrial application is much required for future applications and much more challenging than the indoor environment. Moreover, one of the main motivations to consider the Málaga (Ḿ) model is generalized, i.e., both log-normal and Generalized-K (also called Gamma-Gamma) models can be viewed as a special case of this general model. In particular, we consider two legitimate peers that wish to communicate securely in the presence of an external observer [28]. In the last two decades, different probability distribution functions (PDFs) have been used extensively by many authors for modeling the different atmospheric turbulence conditions, namely, log-normal for weak turbulence, gamma-gamma for strong and moderate turbulence, and negative-exponential for strong turbulence.

A new direction of research in this area is to use a generalized distribution to include all other well-known distributions for appropriately modeling the ever-changing atmospheric turbulence conditions. Málaga (Ḿ) distribution serves the purpose mentioned above as it has been shown that different distributions like Rice-Nakagami, gamma-gamma, shadowed-Rician, K-distribution, homodyned-K, exponential, Gamma-Rician, etc. can be constructed from Málaga (Ḿ) distribution. Moreover, it suits both simulation and experimental results [28]. We choose the Málaga (Ḿ) channel over other channel models with the mentioned advantage, and it considers both large and small-scale fading. We will try to adopt GBSM or hybrid channel model for outdoor applications in the future.

From the literature mentioned above, it's been clear that outdoor transmission link distance is limited due to AT and PE, SC scheme is neglected in many studies, complexity in analytical modeling especially in MIMO-OFDM system due to Meijer-G function. So to overcome and rectify the above problem statement, we proposed a closed-form PDF in this

work which is power series based for Málaga (Ḿ) channel model to reduce the complexity in analytical modeling. The BER, Asymptotic BER (ABER), complex diversity and combining gain analysis are obtained from the proposed PDF. The LDPC coding is also used to enhance the proposed MIMO-OFDM-based FSO link's performance and $M-ary\ QAM$ modulation technique. To the authors' knowledge, the evaluation of MIMO-OFDM with a combination of $M-ary\ QAM$ and Málaga (Ḿ) channel model with PE and AT for all three combining schemes is not yet analyzed with LDPC. To understand the real-time scenario, the study of the FSO link, with the effect of PE and AT factors should be considered with the combining techniques.

The rest of the paper is as follows. The FSO link design, distribution model, PDF expression, and BER analysis are discussed in Section II. The analytical modeling of BER and ABER of MIMO with OFDM based FSO link is derived in Section III. The outage probability and asymptotic BER in section IV and V. The detailed encoding and decoding of the LDPC technique is described in Section VI. The combining gain advantage δG (N, M) for MRC over EGC and SC is discussed in section VII. The obtained numerical results and performance evaluation are discussed in Section VIII before the conclusion in Section IX.

II. FSO DESIGN

A. BLOCK DIAGRAM

Fig.1 gives the working model of the proposed MIMO/FSO link with OFDM and LDPC coding technique with three sections. Section A is transmitter part i.e., from LDPC encoder to laser source $(1, \ldots, N)$, section B is FSO channel and finally section C is receiver i.e., from photo detector to QAM demodulator.

1) SECTION A: TRANSMITTER

The binary data is fed to the LDPC encoder, in which it encodes the input bits before modulating it using $M-ary\ QAM$ modulation. The binary data in serial form are converted to N_P parallel data streams based on the number of laser diodes used one at a time. The data streams in serial are converted to parallel data streams based on number of sub-carriers (M_F) and laser diodes used in the MIMO-OFDM link.

The IFFT is used for summation of all M_{IFFT} sinusoids and provide the easiest way to modulate data using sub-carriers. The M_{IFFT} output samples from IFFT generate a single OFDM symbol. The cyclic prefix is inserted to provide guard interval, eliminating the interference between the previous OFDM symbols and inter –carrier interference (ICI). The RF up-converter converts the low-frequency to high-frequency signals mainly used for point-to-point and satellite communications (SATCOM). The digital to analog (DAC) converts the binary digital data to an analog signal and passes over the atmosphere with N laser diodes for signal transmission after the up-conversion.

2) SECTION B: CHANNEL MODEL

After passing through the fading channel, the transmitted signal will be received using N_{PD} number of photo-detectors (PD) and converted back an analog signal to binary digital data using an analog to digital converter (ADC). With the RF down counter and removal of CP, the data will again permute from serial to parallel based on the total number of sub-carriers.

The receiver side must separate the components and demodulate them. The FFT converts the time domain to the frequency domain, commonly called as de-multiplexing. The parallel to serial converter is used to make them back as single bit steam again.

3) SECTION C: RECEIVER

The signal from the receiver (PD) is combined using combiner schemes like maximal ratio combing (MRC), equal gain combining (EGC), and selection combining (SC).The combiner is used to combine the multiple signals received to improve a single signal. After the combiner, the data bits are converted to serial stream. The LDPC decoder decodes the serial data and $M-ary\ QAM$ demodulator fetches the original input data.

B. SYSTEM MODEL

1) Step1: I/P DATA WITH M-ary QAM

The M-transmitter and N-receiver with SIM based $M-ary\ QAM$ symbol (x) for FSO link is considered under strong AT regime with Additive White Gaussian Noise (AWGN). The j-th receiver aperture's signal output $y(x)$ with η and after FFT it is obtained as follows with nth received symbol of mth sub-carrier received at jth antenna.

$$y(x) = \eta \sum_{i=1}^{M} \left(h_{j,i}(x)\right).r_i(1 \ldots .M_F) + e_i(x) \quad j = 1, 2 \ldots .N \tag{1}$$

Here, $i = 1, 2, \ldots, M$ (transmitter antenna) and $j = 1, 2, \ldots, N$ (receiver antenna) the η optical to electrical converter; with zero mean variance (σ^2) the AWGN is e_i at j-th receiver input; $\boldsymbol{h}_{j,i}(x)$ is irradiance of the transceiver (M, N) apertures at sub-carrier m with average SNR ($\widetilde{\Upsilon}$). The MRC, EGC and SC are the three schemes used here in receiver side to combine the electrical signal. Here, $m = 1 \ldots .M_F$, is the number of sub-carriers, r_i $(1 \ldots . M_F)$ is TX column vector coefficient for real numbers at mth sub-carrier and nth OFDM symbol. In order to demodulate i-th TX signal and j-th RX electrical signal, the combiner is used with three different schemes. Where, x is defined as QAM modulated signal as follows,

$$x(t) = S_I(t)\, Cos(2\pi f_c t) - S_Q(t)\, Sin(2\pi f_c t) \tag{2}$$

Here, In-phase signal carrier signal is $S_I(t) = \sum_{i=-\infty}^{\infty} a_i.g(t - iT_s)$ and Quadrature carrier signal is $S_Q(t) = \sum_{j=-\infty}^{\infty} b_i.g(t - jT_s)$ in which a_i and b_j are amplitude signal and T_s is time interval (symbol interval). Here the two carriers

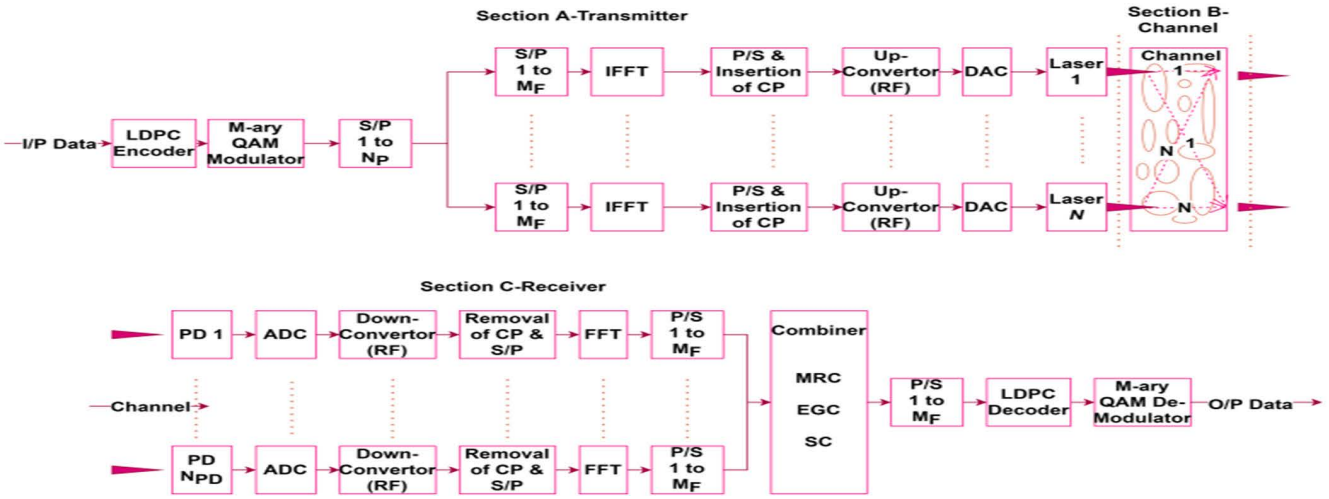

FIGURE 1. A). Transmitter, B). Channel model and C). Receiver for MIMO-OFDM based FSO link with LDPC code.

are taken as in-phase (I) and Quadrature (Q) components and represented as cosine and sine because of 90^0 phase shift with each other. Similarly, i and j are real and imaginary co-ordinates.

The $M-ary\ QAM$ modulates the electrical signal and the intensity of the laser at the TX side; hence the transmitted photocurrent signal is presented as follows

$$S(t) = P_s\left\{1 + k\left[S_I(t)\,Cos(2\pi f_c t) - S_Q(t)\,Sin(2\pi f_c t)\right]\right\} \tag{3}$$

Here, P_s is average TX optical power per symbol, modulation index is k and must satisfy the condition $0< \{1+k.x(t)\} \leq 1$. The instantaneous received electrical SNR for the proposed FSO communication is denoted as follows,

$$\Upsilon = \mu \sum_{i=1}^{M} {h_{j,i}}^2 \tag{4}$$

where, $\mu = \frac{n^2[h^2[\alpha(t)]}{\sigma^2}$ is the average electrical SNR, $h_{j,i}$ is channel co-efficient (assumed to follow $M-ary$ distribution) and variance is σ^2.

2) STEP2: MÁLAGA (Ḿ) CHANNEL

In this work the Málaga (Ḿ) channel model is considered under strong atmospheric turbulence and it used widely for all AT conditions (weak to strong) and competent for characterizing most of the existing channel model like Gamma-Gamma, Log-normal, K-distribution, negative exponential models [9], [29]–[31]. The Málaga (Ḿ) distribution model is used primarily in strong AT [32] and along with PEs and AT is as follows [33],

$$f_{h_{j,i}}(x) = A\sum_{j=1}^{\beta} a_j x^{\frac{a+j}{2}-1}.k_{\alpha-j}\left(2\sqrt{\frac{\alpha\beta x}{g\beta+\Omega'}}\right) \tag{5}$$

Here, the definition of A and a_j is as follows

$$A \triangleq \frac{2\,\propto^{\propto/2}}{g^{1+\frac{\propto}{2}}\mathbb{\Gamma}(\alpha)}\left(\frac{g\beta}{g\beta+\Omega'}\right)^{\beta+\alpha/2} \tag{6}$$

$$a_j \triangleq \left(\binom{\beta-1}{j-1}\frac{(g\beta+\Omega')^{1-\frac{j}{2}}}{(j-1)!}\left(\frac{\Omega'}{g}\right)^{j-2}\left(\frac{\propto}{\beta}\right)^{\frac{j}{2}}\right. \tag{7}$$

The α and β are scintillation parameters, the Gamma function is $\mathbb{\Gamma}(.)$, the modified Bessel function of 2^{nd} order is K, $\binom{\beta}{j}$ is the binomial coefficient, $g = 2b_0(1-\rho)$ is the average power received by off-axis eddies from the scattering components. The term $2b_0$ is total scattering component's average power. The ρ factor introduces amount of scattered power which ranges between 0 and 1. The Ω' parameter represents average power from coherent contributions and is given as follows [34].

$$\Omega' = \Omega + \rho 2b_0 + 2\sqrt{2b_0\Omega_\rho}Cos(\Phi_A - \Phi_B) \tag{8}$$

Here, Ω line of sight (LOS) component average power, (Φ_A, Φ_B) is angles of LOS component. The pointing errors which occurs mainly due to the misalignment between transmitter and receiver plays vital role in reliability and link performance. The pointing error [32] at the receiver side is $I_p = T_O e^{\wedge}((-2r_e^2)/w_a^2)$, with $r_e \geq 0$, $0 \leq I_p \leq T_O$. Here, $T_O = erfc^2(V)$, $V = \frac{\sqrt{\frac{\pi}{2}}R_e}{W_b}$, the error function is erfc, receiver radius is R_e, W_b is size of the received beam.

3) STEP: 3: PROPOSED MÁLAGA (Ḿ) CHANNEL MODEL BASED PDF

The Bessel function i.e., the second term in (5) gets transform in terms of Meijer –G function while expanding the analytical study and termed as follows,

$$f_{h_{j,i}(x)=\frac{A}{2}\sum_{j=1}^{\beta} b_j x^{-1} G_{1,2}^{2,0}\left(\frac{\alpha\beta x}{g\beta+\Omega'}\right)} \tag{9}$$

Here $G_{p,q}^{m,n}(.)$ is Meijer-G function and $b_j = a_j (\frac{\alpha\beta x}{g\beta+\Omega'})^{-\alpha+j/2}$. So based on the (9) the Meijer-G function can be presented as (10) using Slater's theorem.

The Meijer–G function gives complexity in analytical designing of the FSO link especially with MIMO. As a solution a new mathematically tractable PDF with power series is proposed with Málaga (Ḿ) distribution model and PE. It reduces the complexity and moreover used to obtain combining and diversity gain of MIMO/FSO link.

$$
\begin{aligned}
&G_{1,2}^{2,0}\left(\frac{\alpha\beta x}{g\beta+\Omega'}\,|\,\alpha,i\right)\\
&\quad=\mathbb{\Gamma}[j-\alpha]\left(\frac{\alpha\beta x}{g\beta+\Omega'}\right)^{\alpha}\cdot{}_0F_1\left[(1+\alpha-j);\frac{\alpha\beta x}{g\beta+\Omega'}\right]\\
&\qquad+\mathbb{\Gamma}[\alpha-j]\left(\frac{\alpha\beta x}{g\beta+\Omega'}\right)^{j}\cdot{}_0\\
&\qquad\times F_1\left[(1-\alpha+j);\frac{\alpha\beta x}{g\beta+\Omega'}\right]
\end{aligned}
\tag{10}
$$

Here, ${}_pF_q[a_j; b_q; z]$ is generalized Hypo-geometric function, the Gamma function of α is $\mathbb{\Gamma}(\alpha)$ and Gamma function of β is $\mathbb{\Gamma}(\beta)$, g is average power received by off-axis eddies from the scattering components.

The scintillation factors (α, β) which defines the fluctuation of irradiance of the AT is considered as follows. The atmospheric turbulences is defined based on α and β value

$$
\alpha=\frac{1}{exp\left[\frac{0.49\sigma^2}{(1+1.11\sigma_R^{12/5})^{7/6}}\right]-1} \tag{11}
$$

$$
\beta=\frac{1}{exp\left[\frac{0.51\sigma^2}{(1+0.69\sigma_R^{12/5})^{5/6}}\right]-1} \tag{12}
$$

where, $\sigma_R^2 = 1.23\ Cn^2\ k^{7/6}L^{11/6}$ is the irradiance variance, $k = 2\pi/\lambda$, λ is the optical wave number, L is the link distance (meters), Cn^2 is the refractive index structure parameter. The atmospheric turbulence (AT) is differentiated as weak ($C_n^2 = 10^{-17}m^{-2/3}$), moderate ($C_n^2 = 10^{-14}m^{-2/3}$) and strong ($C_n^2 = 10^{-13}m^{-2/3}$) based on the atmospheric structure co-efficient (C_n^2-refractive index) of the ground height greater than 18.6m. We considered the strength of AT based on α and β values as follows: weak ($\alpha = 9$, $\beta = 8$), moderate ($\alpha = 4$, $\beta = 1.9$) and strong ($\alpha = 4.2$, $\beta = 1.2$).

From (10) and (9) with (5) we get (13), after the Laplace transforms and algebra with the power series representation given below

$$
{}_1F_2[a_1 : b_1, b_2 : z]=\sum_{k=0}^{\infty}\frac{(a_1)_k}{(b_1)_k(b_2)_k}\cdot\frac{z^k}{k!} \tag{13}
$$

Here, $(a_1)_k$, $(b_1)_k$ $(b_2)_k$ are defined as Poch-hammer symbols

$$
\begin{aligned}
&{}_0F_1[(1-\alpha+j);\frac{\alpha\beta x}{g\beta+\Omega'}]\\
&\quad=\sum_{k=0}^{\infty}\frac{1}{(1-\alpha+j)_k.k!}\left(\frac{\alpha\beta x}{g\beta+\Omega'}\right)^{k};\\
&\qquad\times{}_0F_1[(1+\alpha-j);\frac{\alpha\beta x}{g\beta+\Omega'}]\\
&\quad=\sum_{k=0}^{\infty}\frac{1}{(1+\alpha-j)_k.k!}\left(\frac{\alpha\beta x}{g\beta+\Omega'}\right)^{k}
\end{aligned}
\tag{14}
$$

Here, $(\alpha)_k$ stands for Pochhammer symbol, based on (10) and (13), after some algebra the Málaga (Ḿ) channel in terms of power series is presented as follows. Let us use the power series representation as follows

$$
\begin{aligned}
f_{h_{j,i}}(x)&=\sum_{j=1}^{\beta}\sum_{k=0}^{\infty}C_{k1}(\propto,j).x^{(k+\propto-1)}\\
&\quad+\sum_{j=1}^{\beta}\sum_{k=0}^{\infty}C_{k2}(\propto,j).x^{(k-j-1)}
\end{aligned}
\tag{15}
$$

Here,

$$
\begin{aligned}
C_{k1}(\propto,j)&=\frac{Ab_j\mathbb{\Gamma}[j-\alpha]}{2(1-\alpha+j)_k k!}.\left(\frac{\alpha\beta x}{g\beta+\Omega'}\right)^{k+\alpha};\\
C_{k2}(\propto,j)&=\frac{Ab_j\mathbb{\Gamma}[a-j]}{2(1-a+j)_k k!}\left(\frac{\alpha\beta x}{g\beta+\Omega'}\right)^{k-j}
\end{aligned}
\tag{16}
$$

The PDF of $(h_{j,i})^2$ is computed from (16), by varying the variable techniques as follows

$$
\begin{aligned}
f_{(h_{j,i})^2}(x)&=\sum_{j=1}^{\beta}\sum_{k=0}^{\infty}\frac{C_{k1}(\propto,j)}{2}.x^{\frac{k+\propto}{2}-1}\\
&\quad+\sum_{j=1}^{\beta}\sum_{k=0}^{\infty}\frac{C_{k2}(\propto,j)}{2}.x^{\frac{k+j}{2}-1}
\end{aligned}
\tag{17}
$$

The PDF of $h_{j,i}$ in terms of PE, α and β, is obtained as follows with $x = I$. The AT and PEs with distribution of $h_{j,i}$ is observed in [35] and using Slater theorem the Meijer-G function with Málaga (Ḿ) model (5) along with PEs equation is simplified and obtained as (18), shown at the bottom of the page.

$$
\begin{aligned}
f_{h_{j,i}}(I)&=\frac{\alpha\beta\xi^2}{A_0\mathbb{\Gamma}(\alpha)\mathbb{\Gamma}(\beta)}\left[\mathbb{\Gamma}\left(\alpha-\xi^2\right)\mathbb{\Gamma}\left(\beta-\xi^2\right)\left(\frac{\beta.I.\alpha}{A_o}\right)^{\xi^2-1}*1\right.\\
&\quad+\frac{\mathbb{\Gamma}(-\alpha+\beta)\mathbb{\Gamma}\left(-\alpha+\xi^2\right)}{\mathbb{\Gamma}\left(1+\xi^2-\alpha\right)}\left(\frac{\alpha\beta I}{A_0}\right)^{-1+\alpha}\sum_{m=0}^{\infty}\frac{\left(\alpha-\xi^2\right)_n}{\left(1+\alpha-\xi^2\right)_n(1+\alpha-\beta)_n}.\frac{\left(\frac{\alpha\beta I}{A_0}\right)^n}{n!}\\
&\quad\left.+\frac{\mathbb{\Gamma}\left(\xi^2-\beta\right)\mathbb{\Gamma}(\alpha-\beta)}{\mathbb{\Gamma}\left(1+\xi^2-\beta\right)}\left(\frac{\alpha\beta I}{A_0}\right)^{\beta-1}\sum_{m=0}^{\infty}\frac{\left(\beta-\xi^2\right)_n}{\left(1+\beta-\xi^2\right)_n(1+\beta-\alpha)_n}.\frac{\left(\frac{\alpha\beta I}{A_0}\right)^n}{n!}\right]
\end{aligned}
\tag{18}
$$

After some algebra and applying (13) in (18) we get the PDF of $h_{j,i}$ (18) in series form is as follows,

$$f_{h_{j,i}}(I) = x_o I^{\xi^2-1} + \sum_{m=0}^{\infty} y_o I^{n+\alpha-1} + \sum_{m=0}^{\infty} z_o I^{n+\beta-1} \tag{19}$$

Here, (19) gets simplified with only two I-exponents of power series compared to Meijer-G in (10). The proposed PDF with PE and AT (18) contains only two power series. So it easy for integral calculation with proposed power series representation compared to complicated function in (10) because it contains only two summations.

4) STEP 4: RECEIVER MODEL (MIMO)

The receiver optical signal is converted to electrical signal using photo detector and formulated as follows

$$r_i(k) = \mu\eta\sqrt{E_g}.P.S[k]\sum_{f=1}^{F} I^{f(t)} + n[k], \quad k = 1, 2, \ldots, k-1 \tag{20}$$

Here, P is average optical power transmitted, η is opto-electro efficiency, modulation index μ, E_g is shaping pulse's energy, $S[k]$ is intensity of atmospheric turbulence channel between TX and RX, $n[k]$ is additive white Gaussian noise. The atmospheric turbulence intensity of the channel is formulated as

$$S[k] = Cos\,\Phi_k - jSin\,\Phi_k \tag{21}$$

The Gaussian noise can be formulated as follows

$$En\{[k].n*[k]\} = 2(\sigma^2) = N_0 \tag{22}$$

5) STEP 5: COMBINER

After receiving the signal from FSO channel, the signal can be combined by combiner using three schemes as follows,

6) MAXIMAL RATIO COMBINING (MRC)

The electrical signal in MRC scheme received is weighted equally with $h_{i,j}(x)$ and γ_{MRC} (i.e., SNR weight-age from TX and RX) from every FSO link which is proportional to the intensity of the every RX [36]. The weighted signals are co-phased and combined coherently to acquire the MRC signal (y_i) as in (23). In [37], the MRC signal is optimal without any interference, nevertheless of the fading statistics the output of the RX with maximal-likelihood technique is obtained as in (25). Nonetheless, the MRC scheme is complex in design but performance is superior because it requires clear proficiency of each link and also sub-carrier phase is required for coherent summation [36] and [37]

$$y_{i(MRC)} = \eta\sum_{j=1}^{N}\sum_{i=1}^{M} h_{j,i}(x).y(x) \tag{23}$$

Here, y(x) is j-th receiver electrical signal. The instantaneous electrical SNR is obtained as follows from (2)

$$\Upsilon_{MRC} = \tilde{\Upsilon}\sum_{j=1}^{N}\left(\sum_{i=1}^{M} h_{j,i}(x)\right)^2 .r_i(1\ldots.M_F) \tag{24}$$

The ML (maximum likelihood) received signal for MRC is as follows:

$$\check{x} = \underset{\tilde{x}\in A}{min}\left|y_i - \eta^2\sum_{j=1}^{N}\left(\sum_{i=1}^{M} h_{j,i}(x)\right)^2 x\right|^2 \tag{25}$$

7) EQUAL GAIN COMBINING (EGC)

In EGC, the $h_{j,i}(x)$ (irradiance) is been collated, phase estimator is used to extract its phase and summed up coherently with equal weight-age of 1 (unity) [36] from N receivers and final EGC signal is framed as in (26). The complexity point of view is less than MRC before weighting the signals received and summation of it. The performance is little bit less than MRC and more or less equal to SC [38]–[40].

$$\begin{aligned} y_{i(EGC)} &= \sum_{j=1}^{N} h_{j,i}(x).y(x) \\ &= \eta\sum_{j=1}^{M}\sum_{i=1}^{N} h_{j,i}(x).r_i(1\ldots.M_F) \\ &\quad + \sum_{j=1}^{N} e_i(x) \end{aligned} \tag{26}$$

From (26), after simplification and some algebra the received SNR is obtained as follows:

$$\Upsilon_{EGC} = \frac{\tilde{\Upsilon}\left(\sum_{j=1}^{N}\sum_{i=1}^{M} h_{j,i}(x)(x)\right)^2}{N} \tag{27}$$

The average SNR $\tilde{\Upsilon}$ is designated as $\tilde{\Upsilon} = \frac{\eta^2 E_x}{\sigma^2}$ from (27).

The ML (maximum likelihood) received signal for EGC is as follows

$$\check{x} = \underset{\tilde{x}\in A}{min}\left|y_i - \eta\sum_{j=1}^{N}\sum_{i=1}^{M} h_{j,i}(x)\right|^2 \tag{28}$$

8) SELECTION COMBINING (SC)

In [41], the SC scheme is considered as less complicated than other combining schemes (MRC and EGC) because it selects the link (i.e., only one receiver from diversity) with high electrical SNR or received irradiance $h_{j,i}(x)$ [10]. The link with good strength or high SNR will be selected after the SC combiner samples all $h_{j,i}(x)$ in view of the fact that noise level for all branches assumed to be equal. Likewise MRC and EGC scheme, the SC scheme not requires any phase estimator for all $h_{j,i}(x)$ [36]. The complexity is reduced due to no phase estimation [36]. The selection made for M links (i = 1, 2, 3 ... M) is obtained as follows

$$y_{(sc)} = max\{SNR(i)\} \tag{29}$$

The SNR of SC combined output is $\tilde{\Upsilon}_{SC} = Max(\tilde{\Upsilon}_1, \tilde{\Upsilon}_2, \tilde{\Upsilon}_3, \ldots..\tilde{\Upsilon}_M)$ and at each branch the average SNR without fading is $\Upsilon_i = \frac{E_b}{\sigma^2}$. The electrical signal is obtained from (1) as follows

$$y_{i(sc)} = \eta\sum_{i=1}^{M}\left(h_{j,i}(x)\right).r_i(1\ldots.M_F) + e_i(x) \tag{30}$$

The output SNR is defined as the ratio of output of the signal power (P_s) to noise power (P_{noise}) and obtained

as follows

$$SNR_{OUTPUT} = \max\left(\frac{P_s}{P_{noise}}\right) \tag{31}$$

The output power of the signal is obtained as follows,

$$P_S = \frac{1}{2}|\eta|^2 \left|\sum_{i=1}^{M}\left(h_{j,i}(x)\right)\right|^2 \tag{32}$$

The output power of the noise is obtained as follows,

$$P_{noise} = \frac{1}{2}|\sigma|^2 \tag{33}$$

The final received SNR can be obtained by substituting (32) and (33) in (31) as follows

$$\Upsilon_{SC} = \bar{\Upsilon}\left(\left(\sum_{i=1}^{M} h_{j,i}(x)\right)^2\right) \tag{34}$$

where, $(\bar{\Upsilon})$ is average SNR and designated as $\bar{\Upsilon} = \frac{\eta^2 E_x}{\sigma^2}$, the SNR of MRC is equal to SNR of the SC under the condition $j = N$.

The ML (maximum likelihood) received signal for SC is as follows:

$$\check{x} = \min_{\tilde{x} \in A} \left| y - \eta\left(\sum_{i=1}^{M} h_{j,i} h_{j,i}(x)\right)^2 x \right|^2 \tag{35}$$

9) STEP 6: POINTING ERROR AND ATMOSPHERIC LOSS

The channel model I_m (combined) is formulated as follows,

$$I_m = I_l . I_a . I_p \tag{36}$$

Here, I_l is atmospheric loss, I_a atmospheric turbulence and I_p is pointing error. Here the atmospheric loss is defined as $I_l = \exp(-\sigma L)$. Where, σ is attenuation co-efficient and L is link length. The atmospheric turbulence denoted with PDF with Málaga (Ḿ) channel model is obtained as follows

$$fI_m(I_m) = A_m \sum_{k=1}^{b} a_{k_m} . I_m^{\frac{a_m+k}{2}-1} . k_{\propto_{m-k}}\left(\sqrt[2]{\frac{\propto_m \beta_m I_m}{\Upsilon\beta_m + \Omega'}}\right) \tag{37}$$

Here,

$$A_m = \frac{2 \propto_m^{\frac{a_m}{2}}}{\Upsilon^{1+\frac{\propto_m}{2}} . \Gamma(\propto_m)} \cdot \left(\frac{\Upsilon . \beta_m}{\Upsilon^{\beta_m + \Omega'}}\right)^{\beta_m + \frac{\propto_m}{2}} \tag{38}$$

$$a_{k_m} = \left(\left(\frac{\beta_m - 1}{k-1}\right) \cdot \frac{\left(\Upsilon\beta_m + \Omega'\right)^{1-\frac{k}{2}}}{k-1!} \cdot \left(\frac{\Omega'}{\Upsilon}\right)^{k-1} \cdot \left(\frac{\propto_m}{\beta_m}\right)^{\frac{k}{2}}\right. \tag{39}$$

The a_m and β_m are positive parameter scattering process and natural number. As surveyed from many literatures the GG channel model is preferred primarily for all AT regime (weak to strong) but not suitable in practical applications. So as mentioned in section I the Málaga (Ḿ) channel model is used widely in recent works because of its perfect suitability in practical applications. The numerical results in [42] define the pointing error as $I_p = T_O e^{\wedge}((-2r_e^2)/w_a^2)$, with $r_e \geq 0$ on the receiver side under the condition $0 \leq I_P \leq T_O$. The T_O is defined as $\text{erfc}^2(V)$, $V = \frac{\sqrt{\frac{\pi}{2}} R_e}{W_b}$, the error function erfc, the radius of the receiver is R_e, W_b is the beam size received. The building sway relation for both horizontal and vertical plane and its relation with variance σ_b^2 and equivalent beam waist w_e is given by [33] as $\xi^2 = w_e^2/4\sigma_b^2$; here $w_e = \left[\sqrt{\pi}\,\text{erfc}(V) W_b^2/(2Ve^{-v^2})\right]^{\frac{1}{2}}$. Pondering the derivations in [33] and [43] the combined channel model of $I_m = I_A I_P$ with AT and PEs is obtained as follows

$$f_{I_M}(I) = \int_{I_A}^{0} f_{\frac{I_M}{I_A}}\left(\frac{I_M}{I_A}\right) . f_A(I_A) . dI_A \tag{40}$$

Here, $f_{\frac{I_m}{I_A}}\left(\frac{I_m}{I_A}\right)$ is the probability in turbulence state I_A. The probability of pointing error I_P is defined as [33]

$$f_P(I_P) = \frac{\xi^2}{A_0^{\xi^2}} I_P^{\xi^2 - 1} \quad 0 \leq I_P \leq A_0 \tag{41}$$

Similarly the definition of $f_{\frac{I_M}{I_A}}\left(\frac{I_M}{I_A}\right)$ is obtained as follows

$$\begin{aligned} f_{\frac{I_M}{I_A}}\left(\frac{I_M}{I_A}\right) &= \frac{1}{I_L . I_A} . f_P(I_P)\left(\frac{I_M}{I_L . I_A}\right) \\ &= \frac{\xi^2}{A_0^{\xi^2} . I_L . I_A}\left(\frac{I_M}{I_L . I_A}\right)^{\xi^2 - 1}, \quad 0 \leq I_P \leq A_0 \end{aligned} \tag{42}$$

By applying (37), (38), (39) and (42) in (40), after simplification and some algebra, the final Probability of PE and AT in terms of power series with combined turbulence effect is as follows,

$$\begin{aligned} f_{I_M}(I) = {} & \frac{\xi^2 . A}{(A_0 . I_L) . \xi^2} . (I_M)^{\xi^2 - 1} * \\ & \times \sum_{k=1}^{b} a_{k_m} \int_{I_M(A_0 I_L)}^{\infty} I_M^{\frac{a_m+k}{2} - 1 - \xi^2} * \\ & \times k_{\propto_{m-k}}\left(\sqrt[2]{\frac{\propto_m \beta_m I_m}{\Upsilon\beta_m + \Omega'}}\right) . dI_A \end{aligned} \tag{43}$$

III. MIMO/FSO PERFORMANCE EVALUATION

A. AVERAGE BER EVALUATION

With the combination of equation (19) and general MGF function [1] we obtained equation (44). Here the independence among $h_{i,j}(x)$ i.e. the MGF of $\sum_{j=1}^{N}\sum_{i=1}^{M} h_{i,j}(x)$ can be written using independence among $h_{i,j}(x)$ as $(M_{h_{i,j}}.(x))^{MN}$. Here i, j have range M, N i.e. $M_{h_{i,j}}.(x)$ in equation (19) the three terms (α, β and ξ^2) is altered with K_1, K_2 and K_3. So in order to reduce the derivation complexity we have taken as K terms $\{K_1(\xi), K_2(\alpha), K_3(\beta)\}$.

The BER can also be computed using the moment generating function (MGF) and it is obtained as follows

$$\varphi_{h_{i,j}^2(s)} = \sum_{j=1}^{\beta}\sum_{k=0}^{\infty}\frac{C_{K1}(\propto,j)}{2} \times \int_0^{\infty} exp(-sx)\, x^{\frac{k+\propto}{2}-1}.dx + \sum_{j=1}^{\beta}\sum_{k=0}^{\infty}\frac{C_{K2}(\propto,j)}{2} \times \int_0^{\infty} exp(-sx)\, x^{\frac{k+j}{2}-1}.dx \quad (44)$$

Here by applying the limit ∞ and expanding, the above integral is calculated as

$$\varphi_{h_{i,j}^2(s)} = \sum_{j=1}^{\beta}\sum_{k=0}^{\infty} C_{K3}(\propto,j).s^{\frac{-(k+\propto)}{2}} + \sum_{j=1}^{\beta}\sum_{k=0}^{\infty} C_{K4}(\propto,j).s^{\frac{-(k+j)}{2}} \quad (45)$$

Here $C_{K3}(\propto,j) = C_{K1}(\propto,j)\,\mathbb{\Gamma}[\frac{k+\propto}{2}]$ and $C_{K4}(\propto,j) = C_{K2}(\propto,j)\,\mathbb{\Gamma}\left[\frac{k+\propto}{2}\right]/2$. The signal from transmitting aperture is assumed to be identical and independently distributed. So the MGF of $\sum_{i=1}^{M} h_{j,i}(x)^2$ is simplified and computed using Binomial theorem applying limit of j as follows

$$\varphi_{h_{i,j}^2(s)} = \sum_{l=0}^{M}\cdot\left(\frac{M}{l}\right)\cdot\left(\sum_{k=0}^{\infty} C_{K3}(\propto,j).s^{\frac{-(k+\propto)}{2}}\right) + \ldots\ldots; +\left(\sum_{k=0}^{\infty} C_{K3}(\propto,\beta).s^{\frac{-(k+\propto)}{2}}\right)^{l} * \times\left(\sum_{k=0}^{\infty} C_{K4}(\propto,1).s^{\frac{-(k+1)}{2}}\right) + \ldots\ldots; + \left(\sum_{k=0}^{\infty} C_{K4}(\propto,\beta).s^{\frac{-(k+\beta)}{2}}\right)^{M-l} \quad (46)$$

So by applying multinomial theorem and convolution, the superscript of $C_k(v)$ is convolved (v-1) times with itself, so (44) gets simplified. The convolution operator and inverse Laplace transform is used to simplify the PDF of $\sum_{i=1}^{M} h_{j,i}(x)^2$ as (47), shown at the bottom of the page.

The average bit error rate of sub-carrier intensity modulation is obtained as follows using the general formula as in [44],

$$P_e(\widetilde{\Upsilon}) = \int_0^{\infty} P_e(\widetilde{\Upsilon}).f_{\widetilde{\Upsilon}}(\widetilde{\Upsilon}).d\widetilde{\Upsilon} \quad (48)$$

The $M-ary\ QAM$ modulation with BER signal-space is defined as follows [44]

$$P_{e(M-aryQAM)}(\Upsilon) = \frac{4}{log_2 M}\left(1-\frac{1}{(\sqrt{M})}\right).\left(\sum_{j=1}^{\sqrt{M}}\Big/ 2Q\left((2i-1)\sqrt{\frac{3E_b log_2 N}{(N-1)\,M_O}}\right)\right. \quad (49)$$

Here, N is number of constellation of $M-ary\ QAM$; Q is q-function. The ABER of $M-ary\ QAM$ with SIM and q-function $Q(x) = \frac{1}{2}erfc(\frac{x}{\sqrt{2}})$ using [1] as follows

$$P_{e(M-QAM)}(\widetilde{\Upsilon}) = \frac{C_m}{2}\sum_{j=1}^{\frac{\sqrt{M}}{2}} Q\left(\frac{\sqrt{\frac{2E_b log_2 M}{N_O(M-1)}}}{\sqrt{2}}\right).f_{\Upsilon}(x).dx \quad (50)$$

Here, $P_e(\widetilde{\Upsilon})$ is PDF based BER expression for Málaga (Ḿ); $f_{\widetilde{\Upsilon}}(\widetilde{\Upsilon})$ is SNR probability function based on Υ and $C_m = \frac{2}{\max(\log_2 M,2)}$ [44]. The Gain and BER expressions are derived and analyzed in terms of power series for all combining schemes. Finally the validation of BER for SIM based $M-ary\ QAM$ modulation and Málaga (Ḿ) channel with M-transmitter is computed as follows by applying (47) and (50) in (48). (51), as shown at the bottom of the page.

The average bit error rate reduces as follows for FSO link with M = 1 (single TX)

$$P_e(\widetilde{\Upsilon}) = \sum_{j=1}^{\beta}\sum_{k=0}^{\infty}\frac{C_{K1}(\propto,j)\,\mathbb{\Gamma}(\frac{k+\alpha+1}{2})}{2.\sqrt{\pi}(k+\alpha)}.\mu^{\frac{-(k+\alpha)}{2}} + \sum_{j=1}^{\beta}\sum_{k=0}^{\infty}\frac{C_{K1}(\propto,j)\,\mathbb{\Gamma}(\frac{k+\alpha+1}{2})}{2.\sqrt{\pi}(k+j)}.\mu^{\frac{-(k+j)}{2}} \quad (52)$$

$$f\sum_{i=1}^{M} {h_{i,j}}^2(x) = \sum_{l=0}^{M}\left(\frac{M}{l}\right) * \times\sum_{\substack{u_1+..+u_\beta=l\\ 0\le u_1,\ldots,u_\beta\le l}}\left(\frac{l}{u_1,\ldots,u_\beta}\right)\sum_{\substack{v_1+..+v_\beta=M-l\\ 0\le u_1,\ldots,u_\beta\le M-l}}\left(\frac{M-l}{v_1,\ldots,v_\beta}\right) \times *\sum_{k=0}^{\infty}\frac{C_K(u,v)}{\left[\frac{k+P}{2}+1\right]}.x^{\frac{(k+P)}{2}} \quad (47)$$

$$P_e(\widetilde{\Upsilon}) = \sum_{l=0}^{M}\left(\frac{M}{l}\right) * \sum_{\substack{u_1+..+u_\beta=l\\ 0\le u_1,\ldots,u_\beta\le l}}\left(\frac{l}{u_1,\ldots,u_\beta}\right)\sum_{\substack{v_1+..+v_\beta=M-l\\ 0\le u_1,\ldots,u_\beta\le M-l}}\left(\frac{M-l}{v_1,\ldots,v_\beta}\right) * \sum_{k=0}^{\infty}\frac{C_K(u,v)\,\mathbb{\Gamma}\left(\frac{k+P+1}{2}\right)}{\mathbb{\Gamma}\left[\frac{k+P}{2}\right].\sqrt{\pi}\,(k+P)}.\mu^{\frac{-(k+P)}{2}} \quad (51)$$

IV. OUTAGE PROBABILITY

The SNR with Cumulative distribution function (CDF) is computed from (53) as follows,

$$F_{\Upsilon}(\Upsilon) = \sum_{l=0}^{M} \binom{M}{l} * \sum_{\substack{u_1 + .. + u_\beta = l \\ 0 \le u_1, \ldots, u_\beta \le l}} \times \binom{l}{u_1, \ldots, u_\beta} \sum_{\substack{v_1 + .. + v_\beta = M - l \\ 0 \le u_1, \ldots, u_\beta \le M - l}} \times \binom{M - l}{v_1, \ldots, v_\beta} * \sum_{k=0}^{\infty} \frac{C_K(u, v)}{\mathbb{\Gamma}\left[\frac{k+P}{2}\right]} \cdot \left(\frac{\Upsilon}{\mu}\right)^{\frac{-(k+P)}{2}} \quad (53)$$

The cumulative density function of received instantaneous SNR for M = 1 reduces as follows

$$f_{\Upsilon}(\Upsilon) = \sum_{j=1}^{\beta} \sum_{k=0}^{\infty} \frac{C_{K1}(\propto, j)}{(k + \alpha)} \left(\frac{\Upsilon}{\mu}\right)^{\frac{k+\propto}{2}} + \sum_{j=1}^{\beta} \sum_{k=0}^{\infty} \frac{C_{K2}(\propto, j)}{(k + j)} \left(\frac{\Upsilon}{\mu}\right)^{\frac{k+j}{2}} \quad (54)$$

The outage probability is the probability which expounded as follows

$$P_{Out}\left(\Upsilon^{th}\right) = F_{\Upsilon}\left(\Upsilon^{th}\right) \quad (55)$$

Therefore the derived power series based PDF is used to calculate the outage probability for different atmospheric turbulences at a given transmission rate.

V. ASYMPTOTIC BER (ABER) ANALYSIS

The ABER expression and average SNR can be computed from (50). The ABER is attained by letting k = 0 in (51) and obtained as follows

$$P_e(\widetilde{\Upsilon}) = \sum_{l=0}^{M} \binom{M}{l} * \sum_{\substack{u_1 + .. + u_\beta = l \\ 0 \le u_1, \ldots, u_\beta \le l}} \times \binom{l}{u_1, \ldots, u_\beta} \sum_{\substack{v_1 + .. + v_\beta = M - l \\ 0 \le v_1, \ldots, v_\beta \le M - l}} \times \binom{M - l}{v_1, \ldots, v_\beta} * \frac{C_0(u, v)\, \mathbb{\Gamma}\left(\frac{P+1}{2}\right)}{\mathbb{\Gamma}\left[\frac{P}{2}\right] \cdot \sqrt{\pi}\,(P)} \mu^{-\frac{P}{2}} \quad (56)$$

The asymptotic outage probability can be achieved with (55) by applying k = 0 as follows

$$P_{Out}\left(\Upsilon^{th}\right) = \sum_{l=0}^{M} \binom{M}{l} * \sum_{\substack{u_1 + .. + u_\beta = l \\ 0 \le u_1, \ldots, u_\beta \le l}} \times \binom{l}{u_1, \ldots, u_\beta} \sum_{\substack{v_1 + .. + v_\beta = M - l \\ 0 \le v_1 + .. + v_\beta \le M - l}} \times \binom{M - l}{v_1, \ldots, v_\beta} * \frac{C_0(u, v)}{\mathbb{\Gamma}\left[\frac{P}{2} + 1\right]} \cdot \left(\frac{\Upsilon^{th}}{\mu}\right)^{\frac{P}{2}} \quad (57)$$

From (56) and (57) the component of μ is (P/2) which has the following conditions [$u_1 + .. + u_\beta = l$, $0 \le u_1, \ldots, u_\beta \le l, v_1 + .. + v_\beta = M - l, 0 \le v_1 + .. + v_\beta \le M - l$].

VI. LOW DENSITY PARITY CHECK (LDPC) CODES

The forward error control (FEC) coding schemes are used widely to detach the errors due to atmospheric factors. Lot of FEC coding techniques has been proposed in literature like Reed-Solomon, Trellis, turbo and Bose–Chaudhuri–Hocquenghem (BCH) codes etc., with the non-linear effects [45] the performance is of LDPC is high compared to other codes in error-prone channels like FSO and fiber optics. LDPC works with parity check matrix and type of linear block codes. The LPDC with generator matrix contains small number of 1's. The LDPC parity matrix (H) of regular code parameters (m, r, t, s) of code rate $k = r/m$ is $(m - r)$ xm matrix. It contains t number of 1's in each column and $s > t$ 1's in each row. Here $t \ll m$, 1's are randomly placed in H, i.e., parity check matrix [46]. The value of $m = 10$, $r = 5$, $t = 2$ and $s = 4$ are considered for our work and it varies with number of bits transmitted. So the number of 1's is obtained as $m.t = (m - r).s$. From this it is easy to show the code rate is 1/2 i.e., $(R = 1 - t/s = 1 - 2/4 = 1/2)$. The uniform 1's in each row and column is the advantage of LDPC coding compared to other techniques. The parity check matrix H with code is generally represented as bipartite graph with check nodes and variables [47]. In LDPC every code bit is considered as variable nodes (a) and check nodes (b) which are represented using parity check. The connection between a and b is obtained when $H_{a,b} = 1$ [48]. Moreover LPDC forms the parity equation based on number of 1's in column and row of the parity matrix. As it is linear block code mechanism encoding policy of LDPC is simple but the decoding part is very complex [49] because count of 1's is quite low in parity check. The message passing decoding algorithm is used in this work [50] along with soft bit decision mechanism [51]. The parameter values are given in Table 1. The steps carried out for generation of bits and reception of MIMO-OFDM based FSO link with LDPC coding is as follows

/// *Step 1:* parameters initialization as r is binary data stream number (n), number of iterations is a, SC_f number of sub-carriers, R number of symbols

/// *Step 2:* LDPC-Parity check matrix

- Initiate with empty matrix and random row should be selected for each column and designate 1's to that column and row.
- Repeat procedure until the number of 1's in that column satisfies the number required for that column.

- Parity check should be made before assigning 1's based on two conditions: the cycle of four girth length should be formed or violation of corresponding row's degree of constraint
- Even if one condition is violated, check again and again by selecting random rows.
- Process should continue until row is found out for the satisfaction of the above constraints together with that column

/// *Step 3: M − ary QAM* modulation and LDPC encoding

- 16-QAM modulation is done and LDPC encoding is performed.

/// *Step 4:* generation of OFDM and encoded signal transmission

- Demultiplexing of signal is performed with IFFT and transferred to channel (atmosphere)

/// *Step 5:* matrix generation of Málaga (Ḿ) channel and addition of AWGN

- The Málaga (Ḿ) channel matrix is generated with accept-reject mechanism and adds AWGN with the signal received.

/// *Step 6:* The signal received will be deducted, demodulated and LDPC decoding

- Received signal is detected and demodulated and bits are decoded using decoding mechanism of LDPC decoder [51]

/// *Step 7:* BER = Total number of errored bits/ transmitted bits in total

- Bit error rate is calculated to observe the coding gain.

VII. COMBINING GAIN δG (N, M) ADVANTAGE OF MRC OVER SC AND EGC SCHEME

Based on the conditions in section V, the diversity gain is computed as follows and here j changes from 1 to β

$$G_{div} = min\left(\frac{P}{2}\right) = \frac{M}{2} min\left(\alpha, j\right) \tag{58}$$

The overall performance gain (δG (N, M)) is theoretically defined as ration of combining gain of MRC over EGC and SC as follows [52]

$$\delta G\left(N, M\right) = \frac{G_{com(mrc)}}{G_{com(egc)}} \tag{59}$$

From the ABER analysis in section V the final combining gain advantage of MRC scheme with EGC is as follows

$$\delta G\left(N, M\right) = \frac{\mathrm{N}.\Gamma\left(2\mathrm{G}_{\mathrm{div(egc)}}/\mathrm{N}\right)^{\mathrm{N}/\mathrm{G}_{\mathrm{div(egc)}}}}{2^{1/\mathrm{G}_{\mathrm{div(egc)}}}.\Gamma\left(2\mathrm{G}_{\mathrm{div(egc)}}\right)^{1/\mathrm{G}_{\mathrm{div(egc)}}}} * \times \frac{\mathbb{\Gamma}\left((\mathrm{G}_{\mathrm{div(mrc)}}\right)^{1/\mathrm{G}_{\mathrm{div(mrc)}}}}{2^{\mathrm{N}/\mathrm{G}_{\mathrm{div(mrc)}}}.\mathbb{\Gamma}\left(\mathrm{G}_{\mathrm{div(mrc)}}/\mathrm{N}\right)^{\mathrm{N}/\mathrm{G}_{\mathrm{div(mrc)}}}} \tag{60}$$

TABLE 1. Parameter values.

Parameter	Values
Atmospheric Turbulence (AT)	Weak AT regime: α=9, β=8; (C_n^2=8.2x10^{-17}m$^{-2/3}$) Moderate AT regime: α=4, β=1.9; (C_n^2=1.5x10^{-14}m$^{-2/3}$) Strong AT regime: α=4.2, β=1.4; (C_n^2=3x10^{-13}m$^{-2/3}$)
MIMO Configuration	M=2,N=2; M=2, N=4; M=4, N=2, M=8, N=4
Pointing error range	Negligible PE :ξ=10.5, 2.15 Strong PE: ξ=0.93 Severe PE: ξ=0.41
No of Subcarriers(M_F)	64
Laser Wavelength (λ)	1550nm
LDPC code rate	1/2
Modulation technique	*M-ary QAM* (16, 32, 64 128)
Link distance	12km

Similarly with SC scheme the combining gain advantage of MRC scheme is follows

$$\delta G\left(\mathrm{N}, \mathrm{M}\right) = \frac{2^{\mathrm{N}/\mathrm{G}_{\mathrm{div(mrc)}}}}{\Gamma.(\mathrm{G}_{\mathrm{div(mrc)}/\mathrm{N}})^{1/\mathrm{G}_{\mathrm{div(mrc)}/(1/\mathrm{N})}}} * \frac{\Gamma.(\mathrm{G}_{\mathrm{div(mrc)}})}{2^{(1/\mathrm{G}_{\mathrm{div(egc)}})}}) \tag{61}$$

From the analysis the MRC provides relative gain of 10log N. The increment in TX and RX gives MRC the superior advantage over SC and EGC (Fig. 7 and Fig. 8).

VIII. RESULTS AND DISCUSSIONS

The characterization of MRC, EGC, and SC schemes for proposed MIMO-OFDM based FSO link with *M − ary QAM* modulation and Málaga (Ḿ) channel model with AT and PEs is discussed in this section. The proposed PDF with power series representation and its derivations in previous sections are used to obtain BER analysis. Simulation results are carried out with MATLAB 2021b under all atmospheric conditions, and the effect of pointing errors is discussed in detail. The mitigation techniques like modulation, MIMO, and coding techniques are incorporated along with the proposed MIMO-OFDM-based FSO link. The proposed derived expressions are taken as K terms to reduce complexity in analytical modeling. The combining and diversity gain, Link distance, outage probability, spectral efficiency, and ergodic capacity are obtained and investigated with PE using the expression derived in previous sections.

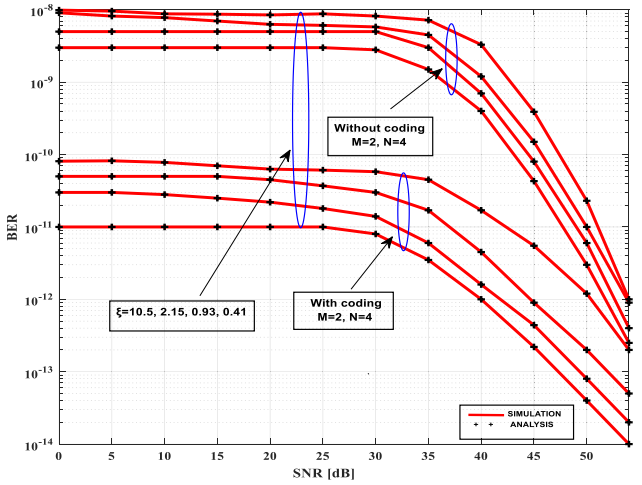

FIGURE 2. Effect of pointing error under weak ($\alpha = 9$, $\beta = 8$) AT regime, M = 2, N = 4, Málaga (Ḿ) channel model, = 10.5, 2.15, 0.93, and 0.41 with $A_0 = 1$.

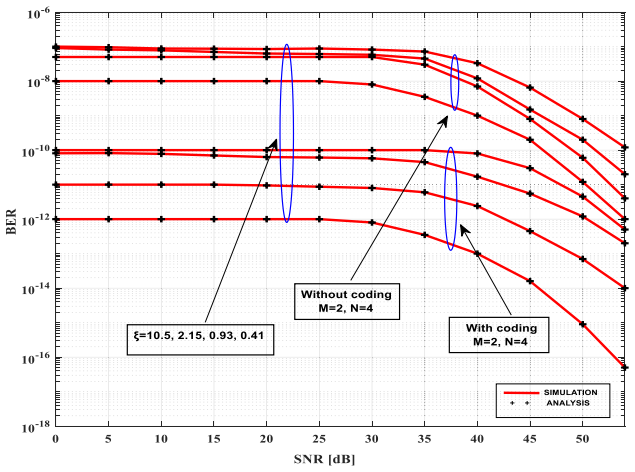

FIGURE 3. Effect of pointing error under moderate ($\alpha = 4$, $\beta = 1.9$) AT regime, M = 2, N = 4, Málaga (Ḿ) channel model, = 10.5, 2.15, 0.93, and 0.41 with $A_0 = 1$.

A. EFFECT OF POINTING ERROR AND ITS MITIGATION USING LDPC IN PROPOSED MIMO-OFDM FSO LINK WITH MÁLAGA (Ḿ) CHANNEL AND COMPARISON OF MIMO/FSO LINK WITH GG CHANNEL

The performance analysis of the proposed MIMO-OFDM based FSO link with $M - ary\ QAM$ modulation with LDPC coding is compared with [52]. The effect of pointing error with LDPC coding and error control under weak, moderate, and strong atmospheric conditions are observed in Fig.2, Fig.3, and Fig.4, respectively. The pointing error of $\xi = 10.5$, 2.15, 0.93, and 0.41 with $A_0 = 1$ is varied to observe the simulated and analytical results in terms of BER vs. SNR which is shown in Fig.2.

The effect of MIMO compared to SIMO [46] and LDPC coding in reduction of error rate is also analyzed and compared with [52] and [53] in Table. 2. The proposed MIMO/FSO link with LDPC coding improves the BER performance and reduces PE's effect compared to the un-coded MIMO/FSO-OFDM link. For weak AT (N = 4, M = 2), without LDPC at ($\xi = 0.41$) i.e. severe PE and negligible PE i.e. ($\xi = 10.5$), the received BER is $\sim 10^{-8.1}$ and $10^{-8.5}$ at 0dB SNR respectively.

Similarly, at 54dB SNR, the BER corresponding to severe PE ($\xi = 0.41$) and negligible PE ($\xi = 10.5$) is 10^{-12} and $10^{-12.7}$ respectively. If we adopt LDPC coding, the BER is observed as 10^{-10} and 10^{-11} at 0dB SNR, $10^{-12.8,}$ and 10^{-14} at 54dB SNR. So the improvement in BER is $10^{-1.9}$ and $10^{-2.6}$ at 0 dB SNR with PE (ξ) 0.41 and 10.5, $10^{-0.8}$ and $10^{-1.3}$ at 54dBSNR, respectively. In [52], for weak AT (N = 4, M = 2), without LDPC at severe PE (ξ) 0.41 and negligible PE of 10.5 the received BER is $10^{-7.5}$ and $10^{-8.2}$ at 0dB SNR respectively similarly, at 54dB SNR the BER corresponding to severe PE ($\xi = 0.41$) and negligible PE ($\xi = 10.5$) is, $10^{-9.7}$ and $10^{-11.8}$ respectively without LDPC. This shows the effectiveness of the LDPC coding with a higher-order modulation technique in the FSO communication link.

The effect of pointing errors in BER is reduced using LDPC coding and the proposed $M - ary\ QAM$/OFDM-based FSO link. The MIMO and LDPC techniques improve the BER of nearly 10^{-6} compared to the MIMO/FSO link [52] without LDPC. It is also observed that the effect of PE is severe with the decrease in ξ value. It is also compared with [53] to study the performance of the MIMO technique. In [53], the SIMO (N = 2, M = 1) with Rician channel gives the BER of $\sim 10^{-1.1}$ and $10^{-1.4}$ only for PE of 0.3(severe) and 8.7(negligible), respectively. It is concluded with MIMO and LDPC, the impact of PE is reduced, even under severe AT. The improvement in BER with LDPC is$\sim 10^{-9}$ compared to [53] and $\sim 10^{-6}$ [52], shown in Table 2.

Similarly, Fig.3 and Fig.4 gives BER performance under moderate and strong AT condition, and the effect of PE is compared with [52]. For moderate AT (N = 4, M = 2), without LDPC coding at severe PE ($\xi = 0.41$) and negligible PE ($\xi = 10.5$) the received BER is $\sim 10^{-7.1}$ and 10^{-8} at 0dB SNR respectively similarly, at 54dB SNR the corresponding BER to severe PE ($\xi = 0.41$) and negligible PE ($\xi = 10.5$) is 10^{-10} and 10^{-12} at respectively.

If we adopt LDPC coding, the BER obtained is 10^{-10} and 10^{-12} at 0dB SNR, $10^{-12.2,}$ and $10^{-16.2}$ at 54dB SNR respectively for N = 4 and M = 2. The BER improvement achieved with the effect of LDPC in the proposed MIMO/FSO-OFDM system is $10^{-2.9}$ and 10^{-4} at 0 dB SNR, $10^{-2.2,}$ and $10^{-4.2}$ at 54dB SNR, respectively for M = 2 and N = 4. In [52] for moderate AT (M = 2 and N = 1), without LDPC coding at severe PE ($\xi = 0.41$) and negligible PE ($\xi = 10.5$) the received BER is 10^{-1} and 10^{-2} at 0 dB SNR respectively, similarly at54dB SNR the corresponding BER to severe PE ($\xi = 0.41$) and negligible PE ($\xi = 10.5$) is $10^{-1.5}$ and $10^{-3.4}$ respectively.

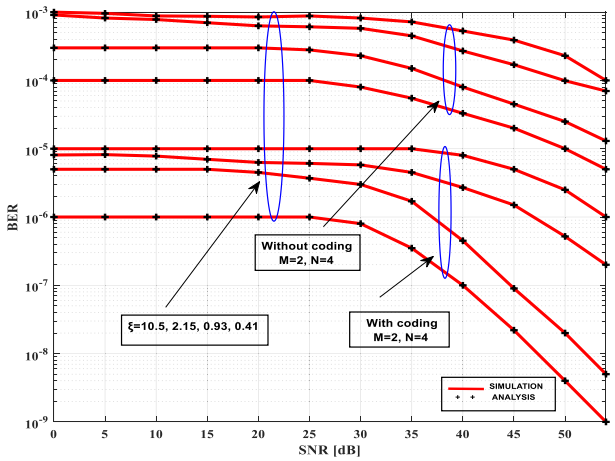

FIGURE 4. Effect of pointing error under strong AT ($\alpha = 4.2$, $\beta = 1.4$) regime, M = 2, N = 4, Málaga (Ḿ) channel model, = 10.5, 2.15, 0.93, and 0.41 with $A_0 = 1$.

For moderate AT (M = 2 and N = 4), without LDPC coding at severe PE ($\xi = 0.41$) and negligible PE ($\xi = 10.5$) the received BER is 10^{-3} and $10^{-3.8}$ at 0dB SNR respectively, similarly at 54 dB SNR, the corresponding BER to severe PE ($\xi = 0.41$) and negligible PE ($\xi = 10.5$) is$10^{-3.7}$ and $10^{-5.8}$ respectively. Here, compared to weak AT, the BER in AT is degraded (10^{-2}) without LDPC but better than [45] and [53]. The coding gain achieved with LDPC is approximately 10^{-6} to 10^{-7} compared to $\sim 10^{-4}$ in [53] and $\sim 10^{-5}$ in [52]. This shows the effectiveness of the proposed system with LDPC coding. The LPDC reduces the bit error rate of nearly 10^{-3} to 10^{-6} compared to [52] and [53].

For strong AT (N = 4, M = 2), without LDPC coding at severe PE ($\xi = 0.41$) and negligible PE ($\xi = 10.5$) the received BER is $\sim 10^{-3}$ and 10^{-4} at 0dB SNR respectively, similarly, at 54dB SNR the corresponding BER to severe PE ($\xi = 0.41$) and negligible PE ($\xi = 10.5$) is 10^{-4} and $10^{-5.4}$ respectively. If we adopt LDPC coding, the BER obtained is 10^{-5} and 10^{-6} at 0dB SNR, 10^{-6} and 10^{-9} at 54dB SNR, respectively for N = 4 and M = 2. The BER improvement with the effect of LDPC in the proposed MIMO/FSO-OFDM system is 10^{-2} and 10^{-2} at 0 dB SNR, 10^{-2} and $10^{-4.4}$ at 54 dB SNR respectively for M = 2 and N = 4. In [45] for strong AT (N = 1, M = 2), without LDPC coding at severe PE ($\xi = 0.41$) and negligible PE ($\xi = 10.5$) the received is 10^{-1} and 10^{-2} at 0 dB SNR respectively, similarly, at 54dB SNR the corresponding BER to severe PE ($\xi = 0.41$) and negligible PE ($\xi = 10.5$) is $10^{-1.5}$ and $10^{-3.4}$ at 54dB respectively.

For moderate AT (M = 2 and N = 4), without LDPC coding at severe PE ($\xi = 0.41$) and negligible PE ($\xi = 10.5$) the received BER is 10^{-3} and $10^{-3.8}$ at 0dB SNR respectively, similarly at 54 dB SNR, the corresponding BER to severe PE ($\xi = 0.41$) and negligible PE ($\xi = 10.5$) is $10^{-3.7}$ and $10^{-5.8}$ respectively. The BER of nearly 10^{-2} to $10^{-2.4}$ is achieved with the proposed system by adopting LDPC coding. Here it is also observed for all PE values (10.5 to 0.41), the corresponding BER is out of desired range (10^{-6} to 10^{-9}) with SIMO and Rician channel model [53]. In [52], the BER is better compared to SIMO link because of the increase in TX and RX and shows the effectiveness of the spatial diversity. As discussed above, the proposed work with LDPC improves the system gain compared to previous work [52].

The proposed system with LDPC coding can obtain the desired BER range even in a strong AT regime under severe PE. This shows the effectiveness of LDPC along with spatial diversity. So it is also recommended that PE maintain higher than 2 (i.e., $\xi > 2$) to acquire the desired BER. In the SIMO link [53], the SNR loss is 2dB at 10^{-4} BER and remains the same for all SNR values with a BER of 10^{-2}. The high SNR of 54dB is achieved with LDPC coding, and $M - ary\ QAM$/OFDM-based proposed FSO link. The little bit degradation in BER of $\sim 10^{-4}$ under strong AT compared to weak and moderate AT, but the coding gain of 10^{-6} to 10^{-7} is achieved with LDPC coding compared to 10^{-2} without LDPC coding [52]. It has been observed that BER is improved with an increase in the number of transmitters, receivers, LDPC coding, and Málaga (Ḿ) channel with $M - ary\ QAM$/OFDM, which is highly reliable under all AT regimes.

The impact of coding with the proposed MIMO-OFDM based FSO link with power series representation is compared with [52] and [53] and tabulated in Table. 2.

The BER analysis of MRC, SC, and EGC for proposed MIMO/FSO link with $M - ary\ QAM$ modulation and Málaga (Ḿ) distribution model with PEs under strong atmospheric turbulence is discussed. The analytical results are obtained from the theoretical derivation done in section II. The BER expressions with the proposed PDF are taken as K-terms to reduce the complexity in BER analysis.

The $M - ary\ QAM$/OFDM modulation and Málaga (Ḿ) distribution model-based MIMO/FSO with $\alpha = 4.2$, $\beta = 1.4$ (strong AT regime) and PEs is shown in Fig. 5 for all three combining schemes with LDPC. The pointing error (ξ) is taken as 10.5(negligible) and 0.41(severe) with $A_0 = 1$.

From Fig.5, it is observed that the simulation and theoretical results match 90%, which verifies the correctness of the derived PDF and analytical expressions in terms of power series. The value of BER increases with an increase in PE. For instance, at severe PE, i.e., 0.41 and above, the BER obtained is $\sim 10^{-2}$ and above for the SC scheme. The BER is not accepted in the desired range for severe PE.

The ξ value needs to be maintained above 1 to acquire the desired BER of 10^{-6} to 10^{-9} and seems tolerable under severe PE ($\xi = 0.42$) with LDPC coding. For example, there is little change in BER, and SNR loss is also bearable under PE of $\xi = 10.5$ and $\xi = 0.4$ for MRC and EGC compared to SC. The SNR corresponding to BER of 10^{-6} and 10^{-7} for $\xi = 0.41$ and, $\xi = 10.5$ the SNR is found to be 10dB in EGC and more than 10dB in SC. It is clear from the figure that MRC outperforms both SC and EGC in terms of SNR loss.

AQ:4 **TABLE 2. Comparative analysis of BER vs. SNR for the proposed work under all AT regime, Málaga (Ḿ), low and severe PEs.**

Proposed work with LDPC						
	Weak AT N=4, M=2		Moderate AT N=4, M=2		Strong AT N=4, M=2	
SNR (dB)	~BER		~BER		~BER	
	ξ=0.9 (strong)	ξ=0.4 (severe)	ξ=0.9 (strong)	ξ=0.4 (severe)	ξ=0.9 (strong)	ξ=0.4 (severe)
0	$10^{-10.1}$	10^{-10}	10^{-10}	10^{-10}	$10^{-5.1}$	10^{-5}
6	$10^{-10.2}$	10^{-10}	$10^{-10.1}$	10^{-10}	$10^{-5.15}$	10^{-5}
16	$10^{-10.3}$	$10^{-10.1}$	$10^{-10.15}$	10^{-10}	$10^{-5.2}$	10^{-5}
26	$10^{-10.4}$	$10^{-10.2}$	$10^{-10.1}$	10^{-10}	$10^{-5.3}$	10^{-5}
36	$10^{-10.6}$	$10^{-10.3}$	$10^{-10.15}$	10^{-10}	$10^{-5.4}$	$10^{-5.1}$
46	$10^{-12.1}$	$10^{-11.2}$	$10^{-10.9}$	$10^{-10.4}$	$10^{-5.8}$	$10^{-5.3}$
54	$10^{-13.5}$	$10^{-12.8}$	$10^{-12.5}$	$10^{-12.2}$	$10^{-6.8}$	10^{-6}
Proposed work without LDPC						
	Weak AT N=4, M=2		Moderate AT N=4, M=2		Strong AT N=4, M=2	
SNR (dB)	~BER		~BER		~BER	
	ξ=0.9	ξ=0.4	ξ=0.9	ξ=0.4	ξ=0.9	ξ=0.4
0	$10^{-8.1}$	10^{-8}	$10^{-7.1}$	10^{-7}	$10^{-3.1}$	10^{-3}
6	$10^{-8.2}$	$10^{-8.1}$	$10^{-7.12}$	10^{-7}	$10^{-3.2}$	$10^{-3.1}$
16	$10^{-8.3}$	$10^{-8.15}$	$10^{-7.13}$	10^{-7}	$10^{-3.3}$	$10^{-3.2}$
26	$10^{-8.5}$	$10^{-8.16}$	$10^{-7.14}$	10^{-7}	$10^{-3.35}$	$10^{-3.21}$
36	$10^{-8.6}$	$10^{-8.2}$	$10^{-7.3}$	$10^{-7.1}$	$10^{-3.4}$	$10^{-3.25}$
46	10^{-10}	$10^{-9.3}$	$10^{-8.8}$	$10^{-8.1}$	$10^{-3.7}$	$10^{-3.4}$
54	$10^{-12.1}$	10^{-12}	$10^{-10.4}$	10^{-10}	$10^{-4.2}$	10^{-4}
Previous work without LDPC [52]						
	Weak AT N=4, M=2		Moderate AT N=4, M=2		Strong AT N=4, M=2	
SNR (dB)	~BER		~BER		~BER	
	ξ=0.9	ξ=0.4	ξ=0.9	ξ=0.4	ξ=0.9	ξ=0.4
0	$10^{-7.5}$	10^{-7}	$10^{-6.41}$	10^{-6}	$10^{-3.2}$	10^{-3}
6	$10^{-7.6}$	$10^{-7.1}$	$10^{-6.5}$	$10^{-6.1}$	$10^{-3.33}$	$10^{-3.1}$
16	$10^{-7.8}$	$10^{-7.3}$	$10^{-6.7}$	$10^{-6.3}$	$10^{-3.36}$	$10^{-3.18}$
26	$10^{-7.9}$	$10^{-7.6}$	$10^{-6.9}$	$10^{-6.4}$	$10^{-3.43}$	$10^{-3.2}$
36	$10^{-8.1}$	$10^{-7.8}$	$10^{-7.1}$	$10^{-6.6}$	$10^{-3.45}$	$10^{-3.3}$
46	$10^{-8.5}$	$10^{-8.2}$	$10^{-7.7}$	$10^{-7.2}$	$10^{-3.6}$	$10^{-3.4}$
54	$10^{-9.7}$	10^{-9}	$10^{-8.7}$	$10^{-8.4}$	$10^{-3.8}$	$10^{-3.6}$
SIMO link with Rician channel model [53]						
	Weak AT, N=2, M=1				Strong AT , N=2, M=1	
SNR (dB)	~BER				~BER	
	ξ=0.9		ξ=0.4		ξ=0.9	ξ=0.4
0	10^{-1}		$10^{-0.8}$		$10^{-0.7}$	$10^{-0.7}$
6	$10^{-1.2}$		$10^{-1.1}$		$10^{-1.1}$	$10^{-0.8}$
16	$10^{-1.5}$		$10^{-1.3}$		$10^{-1.6}$	$10^{-1.1}$
26	$10^{-2.1}$		$10^{-1.4}$		$10^{-1.7}$	$10^{-1.5}$
36	$10^{-2.3}$		$10^{-1.6}$		$10^{-2.2}$	$10^{-1.8}$
46	$10^{-2.5}$		$10^{-1.7}$		$10^{-2.3}$	10^{-3}
54	nil		nil		nil	nil

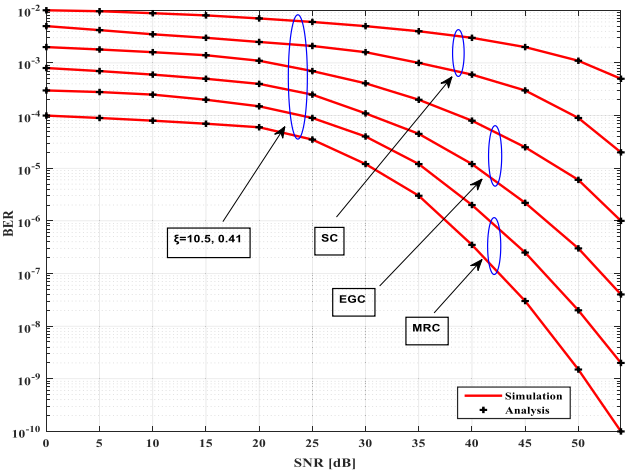

FIGURE 5. BER analysis with *M − ary QAM*, Málaga (Ḿ) distribution, $\alpha = 4.2$, $\beta = 1.4$, $\xi = 10.16, 2.14, 1.45, 1.16, 0.93, 0.41$, $A_0 = 1$ with LDPC for MRC, EGC and SC for M = N = 2.

For example, the SNR loss at BER of 10^{-6} and 10^{-7} for $\xi = 0.41$ is ∼5dB compared with $\xi = 10.5$. It clearly shows with the decrease in ξ value. The SNR gain of ∼5dB and ∼15 dB is achieved compared to EGC and SC.

For strong AT (N = 4, M = 2), with LDPC at severe ($\xi = 0.41$) PE and negligible PE ($\xi = 10.5$), the received BER is $\sim 10^{-3.5}$ and 10^{-4} at 0dB SNR respectively, similarly, at 54dB SNR, the corresponding BER to severe PE ($\xi = 0.41$) and negligible PE ($\xi = 10.5$) is $10^{-8.5}$ and $\sim 10^{-10}$ respectively for MRC. Similarly, for EGC at severe ($\xi = 0.41$) PE and negligible PE ($\xi = 10.5$), the corresponding BER is $\sim 10^{-2.9}$ and $\sim 10^{-3.1}$ at 0dB SNR respectively, similarly, at 54dB SNR, the corresponding BER to severe PE ($\xi = 0.41$) and negligible PE ($\xi = 10.5$) is 10^{-6} and $\sim 10^{-7.2}$ respectively. Similarly, for SC, the corresponding BER is $\sim 10^{-2}$ and $10^{-2.2}$ at 0dB SNR respectively; at 54dB SNR, the corresponding BER to severe PE ($\xi = 0.41$) and negligible PE ($\xi = 10.5$) is $10^{-3.5}$ and $\sim 10^{-5}$ respectively.

The BER with LDPC at severe ($\xi = 0.41$) PE and negligible PE ($\xi = 10.5$) of $10^{-0.6}$ and $10^{-0.9}$, $10^{-1.5}$ and $10^{-1.8}$ is improved with MRC than in EGC and SC at 0dB respectively, similarly at 54dB SNR the corresponding BER improvement to severe PE ($\xi = 0.41$) and negligible PE ($\xi = 10.5$) is $10^{-2.5}$ and $\sim 10^{-2.8}$, $10^{-5.0}$ and $10^{-5.2}$ respectively with MRC.

The BER and SNR loss is also bearable under PE of $\xi = 10.5$ and $\xi = 0.4$ for EGC compared to SC but more or less equal to EGC. The SNR loss at BER of 10^{-6} and 10^{-7} for $\xi = 0.41$ is 10dB approximately compared with $\xi = 10.5$ for EGC and 10dB above for SC. It is clear from the figure that MRC outperforms both SC and EGC in terms of SNR loss. For example, the SNR loss at BER of 10^{-6} and 10^{-7} for $\xi = 0.41$ is 5dB approximately compared with $\xi = 10.5$. It clearly shows that the BER increases rapidly with the decrease in ξ value, 5dB and ∼15 dB SNR gain is achieved compared to EGC and SC. With LDPC the BER obtained at

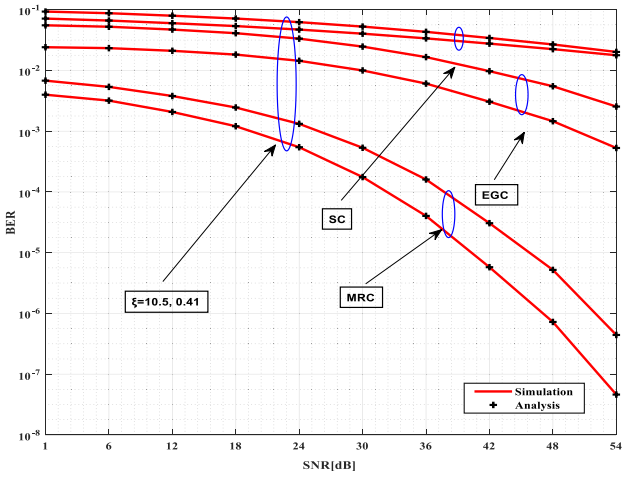

FIGURE 6. BER analysis with $M-ary\ QAM$, Málaga (Ḿ) distribution, $\alpha = 4.2$, $\beta = 1.4$, $\xi = 10.16, 2.14, 1.45, 1.16, 0.93, 0.41$, $A_0 = 1$ without LDPC for MRC, EGC and SC.

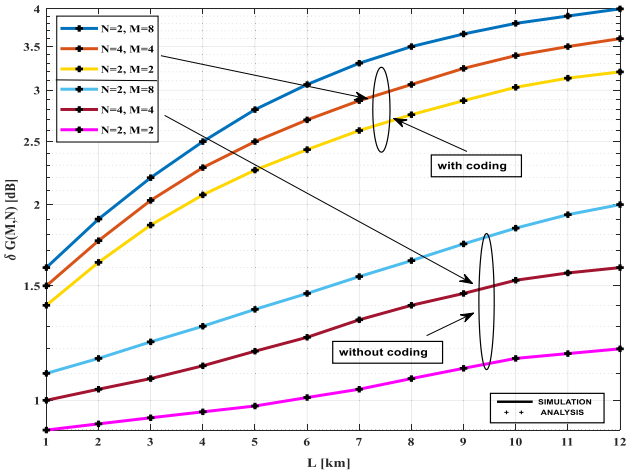

FIGURE 7. Gain analysis δG (N, M) of MIMO/FSO link with1550nm at strong AT ($\alpha = 4.2$, $\beta = 1.4$) for MRC over EGC with link distance (L).

severe PE ($\xi = 0.41$) and negligible PE ($\xi = 10.5$) is $\sim 10^{-3.5}$ and 10^{-4} at 0dB SNR, $10^{-8.5}$ and $\sim 10^{-10}$ at 54dB SNR for M = N = 2 under strong AT for MRC, $\sim 10^{-2.9}$ and $\sim 10^{-3.1}$ at 0dB SNR, 10^{-6} and $\sim 10^{-7.2}$ at 54dB SNR for EGC, $\sim 10^{-2}$ and $10^{-2.2}$ at 0dB SNR, $10^{-3.5}$ and $\sim 10^{-5}$ at 54dB SNR for SC is obtained. The BER of $10^{-0.6}$ and $10^{-0.9}$, $10^{-1.5}$ and $10^{-1.8}$ is getting improved with MRC than EGC and SC at 0dB and $10^{-2.5}$ and $\sim 10^{-2.8}$, $10^{-5.0}$ and $10^{-5.2}$ 54dB SNR for severe PE $\xi = 0.41$) and negligible PE ($\xi = 10.5$).

The performance analysis of EGC, SC and MRC without LDPC coding is shown in Fig.6. For strong AT (N = 4, M = 2), with LDPC at severe ($\xi = 0.41$) PE and negligible PE ($\xi = 10.5$), the received BER is $\sim 10^{-2.1}$ and $\sim 10^{-2.7}$ at 0dB SNR respectively. Similarly, at54dB SNR, the corresponding BER to severe PE ($\xi = 0.41$) and negligible PE ($\xi = 10.5$) is $10^{-6.4}$ and $\sim 10^{-7.4}$ respectively for MRC. Similarly, for EGC at severe ($\xi = 0.41$) PE and negligible PE (ξ =10.5), the corresponding BER is $\sim 10^{-1.2}$ and $\sim 10^{-1.7}$ at 0dB SNR respectively. At 54dB SNR the corresponding BER to severe PE ($\xi = 0.41$) and negligible PE ($\xi = 10.5$) is $10^{-2.5}$ and $\sim 10^{-3.2}$ respectively. Similarly, for SC at severe ($\xi = 0.41$) PE and negligible PE ($\xi = 10.5$), the corresponding BER is $\sim 10^{-1}$ and $10^{-1.2}$ at 0dB SNR respectively, similarly, at 54dB SNR the corresponding BER to severe PE ($\xi = 0.41$) and negligible PE ($\xi = 10.5$) is $10^{-1.7}$ and $\sim 10^{-1.8}$ respectively.

The BER improvement at severe PE ($\xi = 0.41$) and negligible PE ($\xi = 10.5$) of $\sim 10^{-0.9}$ and $\sim 10^{-1}$, $10^{-1.1}$ and $10^{-1.4}$ are achieved with MRC than EGC and SC at 0dB SNR. Similarly, at54dB SNR, the corresponding BER improvement to severe PE ($\xi = 0.41$) and negligible PE ($\xi = 10.5$) is$10^{-3.9}$ and $\sim 10^{-4.2}$, $10^{-4.7,}$ and 10^{-5} respectively for MRC than EGC and SC. From Fig.6 and Fig.7, it is clear that the EGC requires 5 dB extra power to obtain the desired BER range than MRC; similarly, the SC scheme requires extra 15dB power than MRC. Even though with 15dB extra power, the SC scheme cannot obtain the optical BER range with and without LDPC. Without LDPC, only MRC receives the optical BER range. The power required is 15dB and above for EGC and SC, but it cannot attain the desired BER (10^{-6} to 10^{-9}). This shows the effectiveness of the LDPC coding with the proposed MIMO/FSO-OFDM system with $M - ary\ QAM$ modulation and Málaga (Ḿ) distribution.

The BER for all SNR values is compared with [1] and [52] and tabulated in Table. 3. The $M - ary\ QAM$/OFDM, along with the proposed BER expression and Málaga (Ḿ) distribution model, achieves better BER performance compared to M-PSK and QPSK [1] and [52]. For instance, the BER is 10^{0} and $10^{-3.5}$ for QPSK, whereas $10^{-2.6}$ and $10^{-5.4}$ for MPSK at SNR 5dB and 45 dB under severe PEs (PE ($\xi = 0.41$) and strong AT. The SNR gain is nearly 2.3dB. The proposed work with $M - ary\ QAM$ and Málaga (Ḿ) gives $10^{-4.2}$ and 10^{-10} BER for the SNR 5dB and 55 dB compared to SISO and SIMO. The BER achieved is 10^{-3} and SNR gain of $\sim$5-15 dB with MIMO along with $M - ary\ QAM$/OFDM and Malaga (Ḿ) channel compared with SISO/SIMO link [1] and [53]. The proposed system with LDPC gives BER improvement of nearly $\sim 10^{-2}$ to 10^{-3} and $\sim$5 to 15dB SNR gain compared to [52].

The diversity gain analysis δ G (N, M) of MRC over the EGC scheme is analyzed in Fig.7 under a strong AT regime ($\alpha = 4.2, \beta = 1.4$). The ξ, β, and α are obtained from the expressions derived in section II under strong AT. The diversity gain linearly increases for link distance from 1Km to 12Km compared to 8km in [1]. The link distance between TX and RX is increased to 12km compared to 11km and 8km in [1] and [52]. For instance, the MRC gives 3.4 dB gain compared to 2.5dB SNR gain at L = 7km [52] and 3.5dB compared to 2.8dB at 8 Km for N = 4 and M = 8 [52].

TABLE 3. Comparative analysis of ber vs. snr for the work proposed under strong at regime, Málaga (Ḿ), *M − ary QAM*, low and severe PE.

Proposed work with LDPC under AT Regime (strong), M-ary QAM, β=1.4 and α=4.2						
	MRC		EGC		SC	
SNR (dB)	~Bit error rate (dB) ξ=10.5	~Bit error rate (dB) ξ=0.4	~Bit error rate (dB) ξ=10.5	~Bit error rate (dB) ξ=0.4	~Bit error rate (dB) ξ=10.5	~Bit error rate (dB) ξ=0.4
0	10^{-4}	$10^{-3.5}$	$10^{-3.1}$	$10^{-2.9}$	$10^{-2.2}$	10^{-2}
5	$10^{-4.1}$	$10^{-3.6}$	$10^{-3.2}$	$10^{-3.0}$	$10^{-2.3}$	$10^{-2.1}$
10	$10^{-4.2}$	$10^{-3.7}$	$10^{-3.3}$	$10^{-3.1}$	$10^{-2.4}$	$10^{-2.2}$
15	$10^{-4.3}$	$10^{-3.8}$	$10^{-3.4}$	$10^{-3.2}$	$10^{-2.5}$	$10^{-2.3}$
30	10^{-5}	$10^{-4.2}$	10^{-4}	$10^{-3.5}$	10^{-3}	$10^{-2.5}$
45	$10^{-7.8}$	$10^{-6.8}$	$10^{-5.2}$	$10^{-4.3}$	$10^{-3.8}$	$10^{-2.6}$
54	10^{-10}	$10^{-8.8}$	$10^{-7.2}$	10^{-6}	10^{-5}	$10^{-3.5}$
Proposed work without LDPC under AT Regime (strong), M-ary QAM, β=1.4 and α=4.2						
	MRC		EGC		SC	
SNR (dB)	~Bit error rate (dB) ξ=10.5	~Bit error rate (dB) ξ=0.4	~Bit error rate (dB) ξ=10.5	~Bit error rate (dB) ξ=0.4	~Bit error rate (dB) ξ=10.5	~Bit error rate (dB) ξ=0.4
0	$10^{-2.7}$	$10^{-2.1}$	$10^{-1.7}$	$10^{-1.2}$	$10^{-1.2}$	10^{-1}
5	$10^{-2.7}$	$10^{-2.2}$	$10^{-1.8}$	$10^{-1.3}$	$10^{-1.25}$	$10^{-1.1}$
10	$10^{-2.8}$	$10^{-2.3}$	$10^{-1.9}$	$10^{-1.4}$	$10^{-1.3}$	$10^{-1.15}$
15	$10^{-2.9}$	$10^{-2.4}$	$10^{-1.95}$	$10^{-1.45}$	$10^{-1.4}$	$10^{-1.2}$
30	$10^{-3.8}$	$10^{-3.2}$	10^{-2}	$10^{-1.5}$	$10^{-1.5}$	$10^{-1.3}$
45	10^{-6}	10^{-5}	$10^{-2.8}$	$10^{-2.2}$	$10^{-1.6}$	$10^{-1.4}$
54	$10^{-7.4}$	$10^{-6.4}$	$10^{-3.2}$	$10^{-2.5}$	$10^{-1.8}$	$10^{-1.7}$

The maximum gain of 4dB is achieved at 12km with the proposed MIMO-OFDM FSO link with LDPC compared to 2dBwithout LDPC coding. The MRC gives high gain i.e., ∼1dB and 4dB for M = N = 2 and M = 8, N = 4 in the proposed work compared to 1dB and 2.3dB in [1] and [52]. Finally, it's concluded that the performance gain is increased with an increase in transmitters and receivers with LDPC for the proposed system. The coding gain of ∼4 to 6 dB is achieved with the proposed MIMO link along with M-ary QAM and Málaga (Ḿ) channel model compared to 1 and 2 dB in [1] and [52].

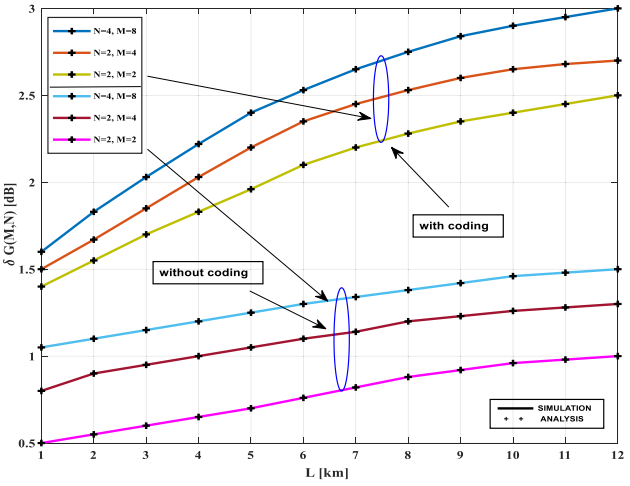

FIGURE 8. Gain analysis δG (N, M) of MIMO/FSO link with1550nm at strong AT ($\alpha = 4.2$, $\beta = 1.4$) for MRC over SC with TX and RX link distance (L).

The diversity gain analysis δG (N, M) of MRC over SC scheme is analyzed in Fig.8 under a strong AT regime. The SNR gain rapidly increases from 1km to 12 km compared to 8Km in [1] but slight performance loss compared to MRC over EGC. The SNR gain is ∼1.2dB and ∼1.5dB for distances 7km and 12Km for without LDPC at M = 8 and N = 4. As the number of transmitters increases, the gain also increases rapidly. For example, the gain of ∼0.5dB and ∼1.2dB is achieved with MRC over SC for M = N = 2 and M = 8, N = 4 at 1km respectively, similarly ∼1dB and ∼1.5dB at 12km without LDPC.

The gain of 0.5dB is less compared with EGC but designing complexity is less. The proposed MIMO/FSO link with LDPC coding increases the link distance from 11km [52] to 12km and a gain of 3dB with the proposed system. The coding gain is nearly doubled compared to [1] and [52]. For instance, at L = 12Km, the MRC gives ∼2.5dB and 3dB for M = 2, N = 2, and M = 8, N = 4. This shows clearly that MRC over EGC attains better gain than MRC over SC with LDPC. Finally, the increase in TX and RX, LDPC, and higher-order modulation techniques like *M − ary QAM* rapidly increases the system's performance compared to the FSO system without LDPC coding. The comparative Table for gain and link distance is observed from [1] and [52] and compared with proposed work for MRC over EGC, which is shown in Table. 4.

Fig.9 shows the spectral efficiency of the proposed system with M = 2 and N = 4 under strong AT condition ($\alpha = 4.2$, $\beta = 1.4$) with1550nm, $Cn^2 = 1.7 \times 10.14 m^{-2/3}$, $W_e/R_e = 11$ and $A_0 = 1$ with severe PE ($\xi = 0.41$). The spectral efficiency is analyzed with and without LDPC, increasing the *M* value of *M − ary QAM* modulation. With LDPC coding, the spectral efficiency achieved is 0, ∼100, and ∼110 bits/Hz/cell at 1dB, 30dB, and 54dB SNR, respectively for M = 16. Similarly 0, ∼120 and ∼140 bits/Hz/cell at 1dB, 30dB and 54dB SNR respectively for M = 128.

TABLE 4. Comparative analysis of performance GAIN ΔG (N, M) vs. L [Km] for the work proposed under strong at regime, Málaga (Ḿ), *M − ary QAM*, low and severe PE for MRC over EGC.

Proposed work with LDPC			Proposed work without LDPC		
AT Regime (strong), M-ary QAM, β=1.4 and α=4.2			AT Regime (strong), M-ary QAM, β=1.4 and α=4.2		
TX/RX	δG(N, M)	L[Km]	TX/RX	δG(N, M)	L[Km]
M=1,N=1	~1	1	M=1,N=1	~1	1
M=2,N=2	~1.8	3	M=2,N=2	~0.6	3
M=1,N=4	~2.0	5	M=1,N=4	~1.0	5
M=2,N=4	~2.8	7	M=2,N=4	~1.4	7
M=1,N=8	~3.8	10	M=1,N=8	~1.8	10
M=4,N=8	~4	12	M=4,N=8	~2	12
Literature [1]			Previous work [52]		
QPSK, AT Regime (strong), β=1.4 and α=4.2 [1]			M-ary PSK, AT Regime (strong), β=1.4 and α=4.2 [52]		
TX/RX	δG(N, M)	L[Km]	TX/RX	δG(N, M)	L[Km]
M=1,N=1	~0	1	M=1,N=1	~0	1
M=2,N=2	~0.3	3	M=2,N=2	~0.3	3
M=1,N=4	~0.6	5	M=1,N=4	~0.8	5
M=2,N=4	~1	7	M=2,N=4	~1.2	7
M=1,N=8	nil	10	M=1,N=8	~1.6	10
M=4,N=8	nil	12	M=4,N=8	nil	12

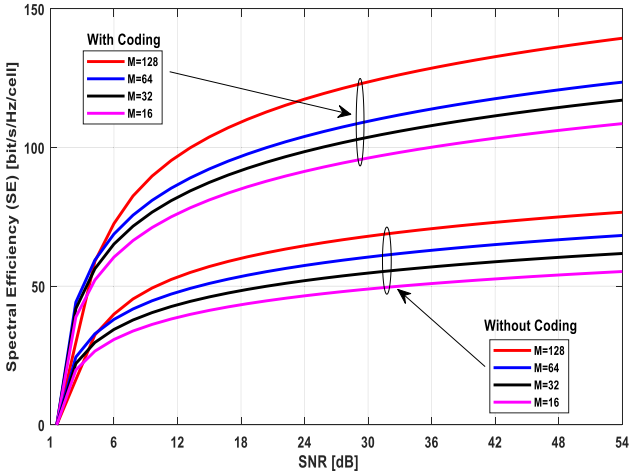

FIGURE 9. Spectral efficiency (SE) vs. SNR for proposed MIMO-OFDM FSO system with N = 4, M = 2, M-QAM, Málaga (Ḿ) and 1550nm under strong AT ($\alpha = 4.2$, $\beta = 1.4$).

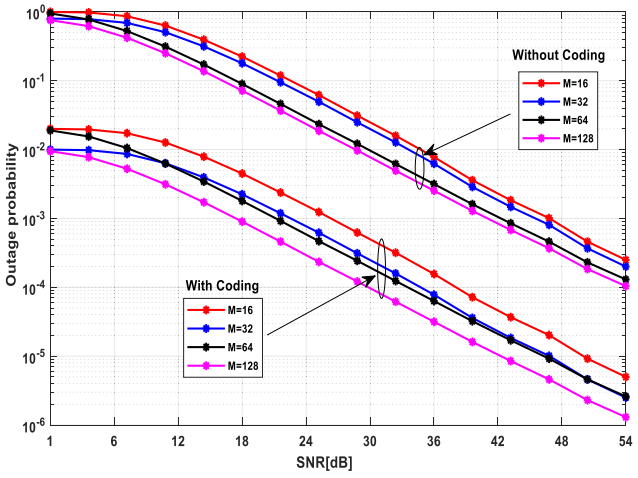

FIGURE 10. Outage probability vs. SNR for proposed MIMO-OFDM FSO system with N = 4, M = 2, M-QAM, Málaga (Ḿ) and 1550nm under strong AT ($\alpha = 4.2$, $\beta = 1.4$). Ergodic capacity vs. SNR for proposed MIMO-OFDM FSO system with N = 4, M = 2, *M − ary QAM*, Málaga (Ḿ) and 1550nm under strong AT ($\alpha = 4.2$, $\beta = 1.4$).

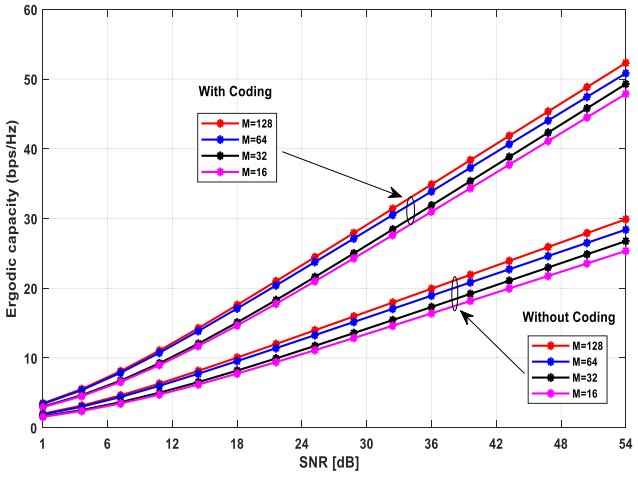

FIGURE 11. Ergodic capacity vs. SNR for proposed MIMO-OFDM FSO system with N = 4, M = 2, M-ary QAM, MMálaga (Ḿ) and 1550nm under strong AT ($\alpha = 4.2$, $\beta = 1.4$).

This shows with an increase in modulation order (M) of the *M − ary QAM* modulation, the spectral efficiency of the proposed system increases. Similarly, it degrades without LDPC coding. For example at M = 16 the SE is ~0, ~30 and ~40 bits/Hz/cell at 1dB, 30dB and 54dB SNR similarly ~0, ~60 and ~70 bits/Hz/cell at 1dB, 30dB and 54dB SNR for M = 128. It is observed from Fig.8 that the spectral efficiency of nearly 70 bits/Hz/cell is improved at M = 128, and 70 bits/Hz/cell is degraded with M = 16. It shows that an increase in the *M −ary QAM* order improves the capacity and efficiency of the proposed MIMO-OFDM based FSO link.

Fig.10 shows the outage probability of the proposed system with M = 2 and N = 4 under strong AT condition ($\alpha = 4.2$, $\beta = 1.4$) with with1550nm, $Cn^2 = 1.7 \times 10.14 m^{-2/3}$, $W_e/R_e = 11$ and $A_0 = 1$ with severe PE ($\xi = 0.41$). The outage probability is analyzed against SNR for M = 16 to 128 modulation orders.

The outage probability starts at 1 dB SNR and reduces rapidly at all SNR values till 54 dB. Here the increase in modulation order reduces the outage probability under severe PE and strong AT regimes. For instance the P_{out} is ~1, $\sim 10^{-2.5}$ and $\sim 10^{-4.2}$ for 1dB, 30 dB and 54 dB SNR respectively for M = 128, similarly at 1dB, 30 dB and 54 dB SNR the

TABLE 5. Overall comparative analysis of proposed work.

Parameters at 55dB SNR and ξ=0.41(severe)	Proposed work		Existing work [52]	Existing work at 45 dB[1]	Existing work at 20dBm [54]
	With LDPC	Without LDPC			
BER under weak AT regime	$\sim10^{-12.8}$	$\sim10^{-12}$	$\sim10^{-9}$	$\sim10^{-5}$	-
BER under moderate AT regime	$\sim10^{-12.2}$	$\sim10^{-10}$	$\sim10^{-8.4}$	$\sim10^{-2.3}$	$\sim10^{-6.3}$
BER under strong AT regime	$\sim10^{-6}$	$\sim10^{-4}$	$\sim10^{-3.6}$	0	$\sim10^{-3.8}$
Gain δG (N, M) of MRC over EGC at M=4,N=8 and L=12Km under strong AT Regime	~4	~2	~2.5	~1.8	-
Gain δG (N, M) of MRC over SC at M=4,N=8 and L=12Km under strong AT regime	~3	~1.5	~1.4	Not done with SC	Not done with SC
Outage probability at strong AT regime and *M-128*	$\sim10^{-6}$	$\sim10^{-4}$	-	-	$\sim10^{-1}$ for 4PPM
Spectral efficiency at strong AT regime and *M-128*	~140bits/Hz/cell	~70 bits/Hz/cell	-	-	-
Ergodic capacity at strong AT regime and *M-128*	~54 bits/Hz/cell	~30bits/Hz/cell			~6 bits/Hz/cell for 4PPM

P_{out} is ∼1, $\sim10^{-1.6}$ and $\sim10^{-3.5}$ respectively for M = 16 without LDPC coding. This shows with an increase in modulation order (M) of the $M-ary\ QAM$ modulation, the outage probability of the proposed system decreases. The proposed system with LDPC coding gives $\sim10^{-2}$, $\sim10^{-4.4}$ and $\sim10^{-6.3}$ for 1dB, 30 dB and 54 dB SNR respectively for M = 128, similarly $\sim10^{-1.8}$, $\sim10^{-3.2}$ and $\sim10^{-5.5}$for 1dB, 30 dB and 54 dB SNR respectively for M = 128. It is concluded from Fig.10 that an increase in modulation order (M) decreases the outage probability, and the coding gain of nearly $\sim10^{-2}$ to $\sim10^{-4}$ is achieved more with the proposed system compared to [54]. This shows the effectiveness of the coding technique in the proposed MIMO-OFDM FSO link.

Fig.11 shows the ergodic capacity of the proposed system with M = 2 and N = 4 under strong AT condition ($\alpha = 4.2$, $\beta = 1.4$) with with1550nm, $Cn^2 = 1.7 \times 10.14$m-2/3, $W_e/R_e = 11$ and $A_0 = 1$ with severe PE ($\xi = 0.41$). The ergodic capacity is analyzed in terms of SNR for M = 16 to 128 modulation orders. Generally, as the M value keeps increasing, the ergodic channel capacity is also increased for all SNR values. The 128-QAM has a larger ergodic channel capacity than 16-QAM under a strong AT regime. Here unlike BER variations, the difference for all QAM is observed under severe PE and strong AT regimes.

The BER is almost vanished in [54], but with the proposed system, it's near the desired BER range. The ergodic capacity achieved is ∼1, ∼12 and ∼25 bits/Hz/cell at 1dB, 30dB and 54dB SNR respectively for M = 16, similarly ∼1.2, ∼15 and ∼30 bits/Hz/cell at 1dB, 30dB and 54dB SNR respectively for M = 128 without LDPC coding.

The proposed FSO link with LDPC gives ∼1.4, ∼25, and ∼47 bits/Hz/cell at 1dB, 30dB, and 54dB SNR, respectively, for M = 16. Similarly ∼1.5, ∼30 and ∼54 bits/Hz/cell at 1dB, 30dB and 54dB SNR respectively for M = 128. Here, the coding gain achieved is near ∼20bits/Hz/cell for 54dB SNR at M = 16, and ∼25 bits/Hz/cell improved at M = 128. So the capacity of ∼25 bits/Hz/cell is achieved more with the proposed system compared to [54].

IX. CONCLUDING REMARKS

The Table. 5 shows the overall comparative analysis of the proposed work, the BER of nearly 10^{-5} to 10^{-7} and gain of 2dB is improved with LDPC coding. Similarly, the outage probability of up to 10^{-5}, spectral efficiency of ∼140bits/Hz/cell and ergodic capacity of ∼48 bits/Hz/cell is improved. This shows the effectiveness of LDPC coding in the proposed MIMO-OFDM/FSO system which are more reliable for future data-hungry applications like IoT, Beyond5G (B5G), Metro applications and so on.

X. CONCLUSION

The complexity of the analytical model is high with the Meijer-G function, especially in MIMO/FSO system. Due to this, the theoretical study with PEs is also complex in MIMO/FSO link. In this paper, the Meijer-G function is simplified, and we proposed a new PDF function based on power series representation for Málaga (Ḿ) and $M-ary\ QAM$ with PEs. The proposed PDF function is used to calculate BER over SNR and performance gain for all combining schemes. We observe the MRC outperforms with a high gain of nearly 5dB and BER of nearly 10^{-6} to 10^{-7} under strong AT. The SC and EGC schemes are acceptable for weak AT and low PEs with slight performance loss in BER than MRC. The SC scheme gives more or less equal gain that of EGC.

The gain, outage probability, efficiency, and capacity of the MIMO/FSO link are improved by mitigating the effect of PE with spatial diversity and coding techniques. The novelty of the work is reducing the complexity of the analytical modeling due to Meijer-G and Bessel of K_{th} order in terms of power series. The correctness of the modeling is verified using MATLAB 2021b. The proposed model is feasible for several SIM-based SIMO and MIMO FSO links which are widely used for 5G, beyond 5G, Smart city applications, satellite, railway and defense applications, etc.,

REFERENCES

[1] M. R. Bhatnagar and Z. Ghassemlooy, "Performance evaluation of FSO MIMO links in gamma-gamma fading with pointing errors," in *Proc. IEEE Int. Conf. Commun. (ICC)*, London, U.K., Jun. 2015, pp. 5084–5090.

[2] D. Kedar and S. Arnon, "Urban optical wireless communication networks: The main challenges and possible solutions," *IEEE Commun. Mag.*, vol. 42, no. 5, pp. S2–S7, May 2004, doi: 10.1109/mcom.2004.1299334.

[3] F. Ahdi and S. Subramaniam, "Optimal placement of FSO relays for network disaster recovery," in *Proc. IEEE Int. Conf. Commun. (ICC)*, Hungary, Hungary, Jun. 2013, pp. 3921–3926.

[4] K. P. Peppas and C. K. Datsikas, "Average symbol error probability of general-order rectangular quadrature amplitude modulation of optical wireless communication systems over atmospheric turbulence channels," *J. Opt. Commun. Netw.*, vol. 2, no. 2, p. 102, Jan. 2010, doi: 10.1364/jocn.2.000102.

[5] W. O. Popoola and Z. Ghassemlooy, "BPSK subcarrier intensity modulated free-space optical communications in atmospheric turbulence," *J. Lightw. Technol.*, vol. 27, no. 8, pp. 967–973, Apr. 15, 2009, doi: 10.1109/jlt.2008.2004950.

[6] T. Ismail, E. Leitgeb, Z. Ghassemlooy, and M. Al-Nahhal, "Performance improvement of FSO system using multi-pulse pulse position modulation and SIMO under atmospheric turbulence conditions and with pointing errors," *IET Netw.*, vol. 7, no. 4, pp. 165–172, Jul. 2018, doi: 10.1049/iet-net.2017.0203.

[7] M. Al-Nahhal and T. Ismail, "Enhancing spectral efficiency of FSO system using adaptive SIM/M-PSK and SIMO in the presence of atmospheric turbulence and pointing errors," *Int. J. Commun. Syst.*, vol. 32, no. 9, p. e3942, Mar. 2019, doi: 10.1002/dac.3942.

[8] M. Al-Nahhal, T. Ismail, H. Selmy, and M. M. Elmesalawy, "BPSK based SIM-FSO communication system with SIMO over log-normal atmospheric turbulence with pointing errors," in *Proc. 19th Int. Conf. Transparent Opt. Netw. (ICTON)*, Girona, Spain, Jul. 2017, pp. 1–4.

[9] E. Bayaki, R. Schober, and R. K. Mallik, "Performance analysis of MIMO free-space optical systems in gamma-gamma fading," *IEEE Trans. Commun.*, vol. 57, no. 11, pp. 3415–3424, Nov. 2009, doi: 10.1109/tcomm.2009.11.080168.

[10] T. A. Tsiftsis, H. G. Sandalidis, G. K. Karagiannidis, and M. Uysal, "Optical wireless links with spatial diversity over strong atmospheric turbulence channels," *IEEE Trans. Wireless Commun.*, vol. 8, no. 2, pp. 951–957, Feb. 2009, doi: 10.1109/twc.2009.071318.

[11] C. Abou-Rjeily, "On the optimality of the selection transmit diversity for MIMO-FSO links with feedback," *IEEE Commun. Lett.*, vol. 15, no. 6, pp. 641–643, Jun. 2011, doi: 10.1109/lcomm.2011.041411.110312.

[12] X. Song and J. Cheng, "Subcarrier intensity modulated MIMO optical communications in atmospheric turbulence," *J. Opt. Commun. Netw.*, vol. 5, no. 9, p. 1001, Aug. 2013, doi: 10.1364/jocn.5.001001.

[13] M. M. Abadi, Z. Ghassemlooy, M.-A. Khalighi, S. Zvanovec, and M. R. Bhatnagar, "FSO detection using differential signaling in outdoor correlated-channels condition," *IEEE Photon. Technol. Lett.*, vol. 28, no. 1, pp. 55–58, Jan. 1, 2016, doi: 10.1109/lpt.2015.2480011.

[14] G. Yang, M.-A. Khalighi, Z. Ghassemlooy, and S. Bourennane, "Performance evaluation of receive-diversity free-space optical communications over correlated gamma-gamma fading channels," *Appl. Opt.*, vol. 52, no. 24, p. 5903, Aug. 2013, doi: 10.1364/ao.52.005903.

[15] I. B. Djordjevic, B. Vasic, and M. A. Neifeld, "LDPC coded orthogonal frequency division multiplexing over the atmospheric turbulence channel," in *Proc. Conf. Lasers Electro-Opt. Quantum Electron. Laser Sci. Conf. (CLEO/QELS)*, Long Beach, CA, USA, 2006, pp. 1–2.

[16] S. Srikanth, P. Sriram, and D. S. Kumar, "Performance analysis of OFDM employing free space optical communication system," in *Proc. 2nd Int. Conf. Electron. Commun. Syst. (ICECS)*, Coimbatore, India, Feb. 2015, pp. 70–74.

[17] Ghassemlooy and Z. Popoola, *Optical Wireless Communication*. New York, NY, USA: CRC Press, 2012.

[18] F. Almasoudi, K. Alatawi, and M. A. Matin, "Study of OFDM technique on RoF passive optical network," *Opt. Photon. J.*, vol. 3, no. 2, pp. 217–224, 2013, doi: 10.4236/opj.2013.32035.

[19] J. Wang, C. P. Udeh, and W. Rangzhong, "Fast QC-LDPC code for free space optical communication," *Proc. SPIE*, vol. 10096, Feb. 2017, Art. no. 1009609.

[20] X. Liu, P. Wang, T. Liu, Y. Li, L. Guo, and H. Tian, "ABER performance of LDPC-coded OFDM free-space optical communication system over exponentiated Weibull fading channels with pointing errors," *IEEE Photon. J.*, vol. 9, no. 4, pp. 1–13, Aug. 2017, doi: 10.1109/jphot.2017.2723427.

[21] M. Sharma, D. Chadha, and V. Chandra, "Performance analysis of MIMO–OFDM free space optical communication system with low-density parity-check code," *Photon. Netw. Commun.*, vol. 32, no. 1, pp. 104–114, Nov. 2015, doi: 10.1007/s11107-015-0579-y.

[22] M. R. Abaza, R. Mesleh, A. Mansour, and A. Alfalou, "MIMO techniques for high data rate free space optical communication system in log-normal channel," in *Proc. Int. Conf. Technol. Adv. Electr., Electron. Comput. Eng. (TAEECE)*, Konya, Turkey, May 2013, pp. 1–5.

[23] M. Sharma, D. Chadha, and V. Chandra, "Performance analysis of spatially multiplexed MIMO-OFDM free space optical communication system," in *Proc. Int. Conf. Signal Process. Commun. (SPCOM)*, Bengaluru, India, Jul. 2014, pp. 1–5.

[24] Y. Wang, D. Wang, and J. Ma, "On the performance of coherent OFDM systems in free-space optical communications," *IEEE Photon. J.*, vol. 7, no. 4, pp. 1–10, Aug. 2015, doi: 10.1109/jphot.2015.2450532.

[25] D. He, K. Guan, J. M. García-Loygorri, B. Ai, X. Wang, C. Zheng, C. Briso-Rodríguez, and Z. Zhong, "Channel characterization and hybrid modeling for millimeter-wave communications in metro train," *IEEE Trans. Veh. Technol.*, vol. 69, no. 11, pp. 12408–12417, Nov. 2020, doi: 10.1109/tvt.2020.3023153.

[26] Q. Zhu, H. Li, Y. Fu, C.-X. Wang, Y. Tan, X. Chen, and Q. Wu, "A novel 3D non-stationary wireless MIMO channel simulator and hardware emulator," *IEEE Trans. Commun.*, vol. 66, no. 9, pp. 3865–3878, Sep. 2018, doi: 10.1109/tcomm.2018.2824817.

[27] N. Avazov, R. Hicheri, M. Muaaz, F. Sanfilippo, and M. Patzold, "A trajectory-driven 3D non-stationary mm-wave MIMO channel model for a single moving point scatterer," *IEEE Access*, vol. 9, pp. 115990–116001, 2021, doi: 10.1109/access.2021.3105296.

[28] A. Das, B. Bag, C. Bose, and A. Chandra, "Free space optical links over Málaga turbulence channels with transmit and receive diversity," *Opt. Commun.*, vol. 456, Feb. 2020, Art. no. 124591, doi: 10.1016/j.optcom.2019.124591.

[29] D. AnandKumar and R. G. Sangeetha, "Performance analysis of power series based MIMO/FSO link with pointing errors and atmospheric turbulence," in *Proc. Int. Conf. Commun. Syst. Netw. (COMSNETS)*, Bengaluru, India, Jan. 2021, pp. 78–81.

[30] K. P. Peppas and C. K. Datsikas, "Average symbol error probability of general-order rectangular quadrature amplitude modulation of optical wireless communication systems over atmospheric turbulence channels," *J. Opt. Commun. Netw.*, vol. 2, no. 2, p. 102, Jan. 2010, doi: 10.1364/jocn.2.000102.

[31] D. Anandkumar and R. G. Sangeetha, "A survey on performance enhancement in free space optical communication system through channel models and modulation techniques," *Opt. Quantum Electron.*, vol. 53, no. 1, pp. 1–39, Nov. 2020, doi: 10.1007/s11082-020-02629-6.

[32] M. Uysal, J. Li, and M. Yu, "Error rate performance analysis of coded free-space optical links over gamma-gamma atmospheric turbulence channels," *IEEE Trans. Wireless Commun.*, vol. 5, no. 6, pp. 1229–1233, Jun. 2006, doi: 10.1109/twc.2006.1638639.

[33] W. Gappmair, "Further results on the capacity of free-space optical channels in turbulent atmosphere," *IET Commun.*, vol. 5, no. 9, pp. 1262–1267, Jun. 2011, doi: 10.1049/iet-com.2010.0172.

[34] K. A. Balaji and K. Prabu, "Performance evaluation of FSO system using wavelength and time diversity over Malaga turbulence channel with pointing errors," *Opt. Commun.*, vol. 410, pp. 643–651, Mar. 2018, doi: 10.1016/j.optcom.2017.11.006.

[35] M. R. Bhatnagar, "A one bit feedback based beamforming scheme for FSO MISO system over gamma-gamma fading," *IEEE Trans. Commun.*, vol. 63, no. 4, pp. 1306–1318, Apr. 2015, doi: 10.1109/tcomm.2015.2391178.

[36] W. O. Popoola, Z. Ghassemlooy, J. I. H. Allen, E. Leitgeb, and S. Gao, "Free-space optical communication employing subcarrier modulation and spatial diversity in atmospheric turbulence channel," *IET Optoelectron.*, vol. 2, no. 1, pp. 16–23, Feb. 2008, doi: 10.1049/iet-opt:20070030.

[37] M. K. Simon and M.-S. Alouini, *Digital Communication Over Fading Channels: A Unified Approach to Performance Analysis*. New York, NY, USA: Wiley, 2000.

[38] A. Annamalai, C. Tellambura, and V. K. Bhargava, "Exact evaluation of maximal-ratio and equal-gain diversity receivers for M-ary QAM on Nakagami fading channels," *IEEE Trans. Commun.*, vol. 47, no. 9, pp. 1335–1344, Sep. 1999, doi: 10.1109/26.789669.

[39] N. C. Sagias, G. K. Karagiannidis, P. T. Mathiopoulos, and T. A. Tsiftsis, "On the performance analysis of equal-gain diversity receivers over generalized gamma fading channels," *IEEE Trans. Wireless Commun.*, vol. 5, no. 10, pp. 2967–2975, Oct. 2006, doi: 10.1109/twc.2006.05301.

[40] G. K. Karagiannidis, "Moments-based approach to the performance analysis of equal gain diversity in Nakagami-*m* fading," *IEEE Trans. Commun.*, vol. 52, no. 5, pp. 685–690, May 2004, doi: 10.1109/tcomm.2004.826255.

[41] M. K. Simon and M.-S. Alouini, *Digital Communication Over Fading Channels: A Unified Approach to Performance Analysis*. New York, NY, USA: Wiley, 2000.

[42] A. A. Farid and S. Hranilovic, "Outage capacity optimization for free-space optical links with pointing errors," *J. Lightw. Technol.*, vol. 25, no. 7, pp. 1702–1710, Jul. 2007, doi: 10.1109/jlt.2007.899174.

[43] H. G. Sandalidis, T. A. Tsiftsis, G. K. Karagiannidis, and M. Uysal, "BER performance of FSO links over strong atmospheric turbulence channels with pointing errors," *IEEE Commun. Lett.*, vol. 12, no. 1, pp. 44–46, Jan. 2008, doi: 10.1109/lcomm.2008.071408.

[44] J. Lu, K. B. Letaief, J. C.-I. Chuang, and M. L. Liou, "M-PSK and M-QAM BER computation using signal-space concepts," *IEEE Trans. Commun.*, vol. 47, no. 2, pp. 181–184, Feb. 1999, doi: 10.1109/26.752121.

[45] I. B. Djordjevic, B. Vasic, and M. A. Neifeld, "LDPC coded orthogonal frequency division multiplexing over the atmospheric turbulence channel," in *Proc. Conf. Lasers Electro-Opt. Quantum Electron. Laser Sci. Conf.*, Long Beach, CA, USA, 2006, pp. 1–2.

[46] B. Lu, G. Yue, and X. Wang, "Performance analysis and design optimization of LDPC-coded MIMO OFDM systems," *IEEE Trans. Signal Process.*, vol. 52, no. 2, pp. 348–361, Feb. 2004, doi: 10.1109/tsp.2003.820991.

[47] X. Liu, P. Wang, T. Liu, Y. Li, L. Guo, and H. Tian, "ABER performance of LDPC-coded OFDM free-space optical communication system over exponentiated Weibull fading channels with pointing errors," *IEEE Photon. J.*, vol. 9, no. 4, pp. 1–13, Aug. 2017, doi: 10.1109/jphot.2017.2723427.

[48] D. J. C. MacKay, "Good error-correcting codes based on very sparse matrices," *IEEE Trans. Inf. Theory*, vol. 45, no. 2, pp. 399–431, Mar. 1999, doi: 10.1109/18.748992.

[49] Z. Fei, J. Yuan, M. Xiao, B. Bai, S. Zhang, and D. Lin, "Recent development of error control codes for future communication and storage systems," *China Commun.*, vol. 14, no. 8, pp. 3–5, Aug. 2017, doi: 10.1109/cc.2017.8014341.

[50] M. czaputa, T. Javornik, E. Leitgeb, G. Kandus, and Z. Ghassemlooy, "Investigation of punctured LDPC codes and time-diversity on free space optical links," in *Proc. 11th Int. Conf. Telecommun. (ConTEL)*, Graz, Austria, 2011, pp. 1–3.

[51] S. B. Rowhani, A. Ghaneizadeh, and I. A. Akhlaghi, "Performance analysis of elastic MIMO-RF/FSO communication over Lutz model with LDPC," in *Proc. 2nd West Asian Colloq. Opt. Wireless Commun. (WACOWC)*, Tehran, Iran, Apr. 2019, pp. 41–45.

[52] D. Anand Kumar and R. G. Sangeetha, "Power series based gamma–gamma fading MIMO/FSO link analysis with atmospheric turbulence and pointing errors," *Opt. Quantum Electron.*, vol. 53, no. 9, pp. 1–27, Aug. 2021, doi: 10.1007/s11082-021-03103-7.

[53] H. Zhou, W. Xie, L. Zhang, Y. Bai, W. Wei, and Y. Dong, "Performance analysis of FSO coherent BPSK systems over rician turbulence channel with pointing errors," *Opt. Exp.*, vol. 27, no. 19, p. 27062, Sep. 2019, doi: 10.1364/oe.27.027062.

[54] S. Magidi and J. A. Afthab, "Performance analysis of multipulse position modulation free space optical communication system under generalized atmospheric turbulence conditions including pointing errors," *Opt. Eng.*, vol. 59, no. 1, p. 1, Jan. 2020, doi: 10.1117/1.oe.59.1.016107.

D. ANANDKUMAR (Member, IEEE) received the Bachelor of Engineering degree in electronics and communication engineering and the Master of Engineering degree in communication systems from Anna University, Chennai, in 2010 and 2012, respectively. He is currently pursuing the dual master's and Ph.D. degree with the Vellore Institute of Technology University, Chennai Campus. His current research interests include free space optical communication, microwave, and digital communication.

R. G. SANGEETHA (Senior Member, IEEE) received the B.E. degree in electronics and communication engineering from Bharathidasan University, Tiruchirappalli, in 1999, the M.E. degree in computer and communication from Anna University, Chennai, in 2005, and the Ph.D. degree from the Indian Institute of Technology, New Delhi. She is currently working as an Associate Professor with VIT University, Chennai. Her research interests include free space optical communication, optical networks, communication systems and semiconductor devices, digital electronics, digital and analog communications, and machine learning.